BSC thesis Applied Earth Sciences
Department of Geosciences and Engineering
Delft University of Technology

Mapping of thin-bedded crevasse-splay deposits in a low-N/G floodplain environment

Huesca fluvial fan, Ebro Basin, Spain

12-07-2014

Marloes Jongerius (4017617)

Supervisors:
Dr. M.E. Donselaar
Dr. G.J. Weltje
Ir. K.A. van Toorenenburg

Contents

Abstract

A good understanding of the reservoir architecture of tough gas reservoirs is necessary to define their potential for the hydrocarbon industry. These tough gas reservoirs have been overlooked until now due to the high economic risks of development. These risks are mainly related to the large uncertainties that exist in the reservoir architecture. Understanding the depositional processes of crevasse-splays will help in minimizing the uncertainties in interpreting the internal depositional setting and deposition processes.

This research focuses on the mapping of thin bedded crevasse splays in a low-net-over-gross floodplain environment in the distal areas of the Huesca fluvial fan (Miocene) of the Ebro basin in Spain. This outcrop is a good analogue to the Permian Rötliegend and Triassic Bundsandstein intervals in the West Netherlands Basin.

A field study of the Huesca fluvial fan is used to analyse the reservoir architecture (size, shape, spatial distribution and connectivity) of the reservoirs of fossil crevasse-splay deposits. At two outcrop locations an interval of crevasse-splay deposits is mapped, using detailed lithostratigraphical logs, a type section log, photo-panels and lateral characterizations of sand beds. With these data a correlation panel is constructed to determine the connectivity of the mapped layers, and cross-sections are made to determine the lateral continuity, vertical stacking and grain-size variations.

On a single layer level, results show both a decrease in bed thickness and in grain size from proximal to distal, related to the energy of deposition. Grain size is also related to distributary-channel proximity, decreasing away from the distributary crevasse channels. In multi-storey stacked sheets, incision of distributary channels into underlying crevasse deposits near the crevasse apex creates sand-on-sand contact. The approximation of a crevasse splay as a simple accumulation of homogeneous sheet like layers should be refined in order to lower the uncertainties in the tough gas reservoir model. A quantitative dataset for the size, shape and stacking patterns of crevasse splay sandstone is composed, which can be used as an input in static reservoir models.

1. Introduction

As conventional gas reservoirs become scarce and the demand for hydrocarbons is still increasing, there is a high demand for additional production from less conventional settings. The unconventional *tough gas* reservoirs, formed by crevasse splay deposits in a low-N/G fluvial floodplain environment, have due to their areal extension and reservoir properties, a high potential to become an additional source of fossil energy in the future. In the Northwest European gas province, the development of *tough gas* may even prolong the hydrocarbon production in mature areas.

However, these reservoirs have been overlooked until now due to the high economic risks of development. These economic risks are mainly related to the large uncertainties that exist in the reservoir architecture. A good understanding of crevasse splays in terms of size, shape, spatial distribution and connectivity of the reservoirs, and low permeability, is crucial to define their new perspective in the hydrocarbon industry. This research is done in order to gain more insight in these uncertain depositional processes.

The distal part of the late Oligocene to early Miocene Huesca fluvial fan terminating on the rim of the Ebro Basin in Spain (Donselaar and Schmidt, 2005), provides outcrops of thin-bedded crevasse splay deposits in a low net-to-gross floodplain environment. The quality and quantity of the exposures makes this a good location for a case study.

A previous study of the Ebro Basin by Nichols and Fisher (2007) shows that when descending to the distal area of the fluvial fan, the channels are decreasing in depth and are eventually terminating at the distal part (Figure 1) of the fluvial fan. River channels commonly terminate in areas where the channel capacity is reduced and floodwaters spread across the alluvial surface forming terminal flood-outs. This process is characterized by a transition from confined to un-confined flow (Nichols and Fisher, 2007). As a consequence there is a distal decrease of the amount of sandstone bodies formed as in-channel deposits and an associated increase of unconfined flow deposits.

This process of increasing unconfined flow can be explained by the dwindling energy of the system. River systems in an arid to semi-arid climate setting in hydrologically-closed basins experience downstream transmission losses by percolation and evapo-transpiration (Donselaar et al., 2013) (Figure 1). As a consequence of the declining amount of water, the energy level will fall. A further energy drop is a consequence of the low gradient of the floodplain area, where the contribution of gravity-driven flow is negligible. Bifurcation of the channel into a radial pattern of branching channels also results in lower flow energy due to the lower volume of water passing through each channel.

As can be seen, from the proximal to distal area of the fluvial fan, the channel size is decreasing and the amount of floodplain deposits is increasing. In the Distal area it is expected to find sheet sandstone, terminal splays, small channels and poorly channelized deposits.

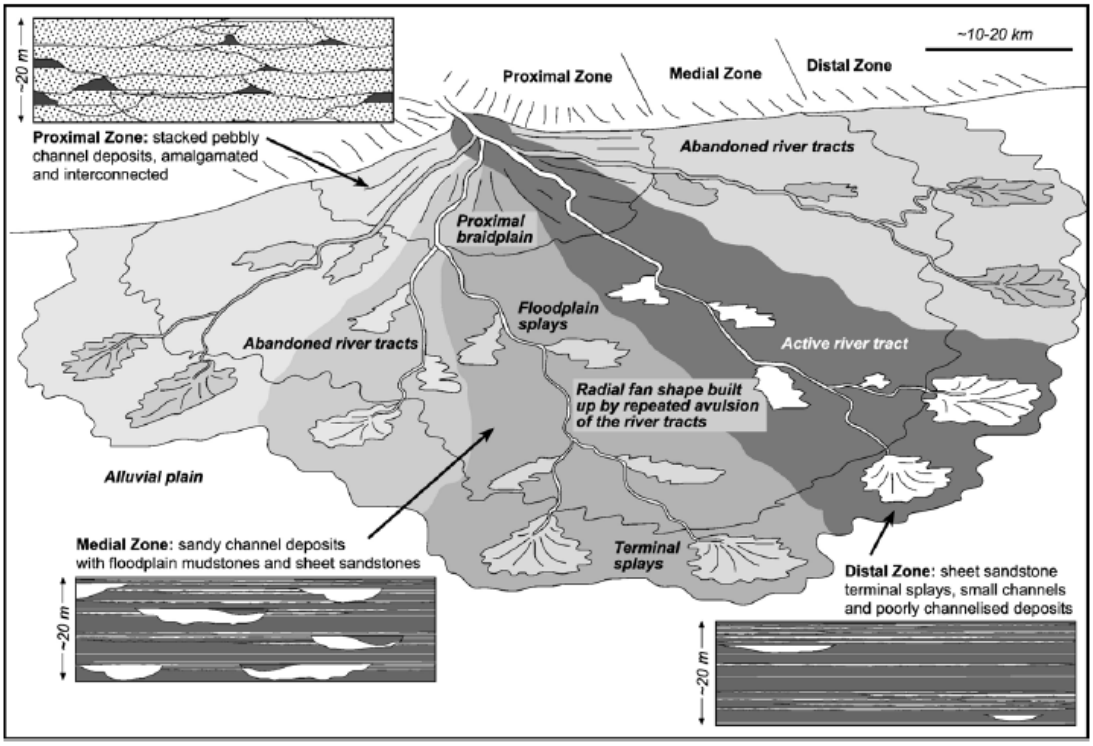

Figure 1. The development of a fan-shaped body of sediments by repeated avulsion of the river channel (from Nichols and Fisher, 2007)

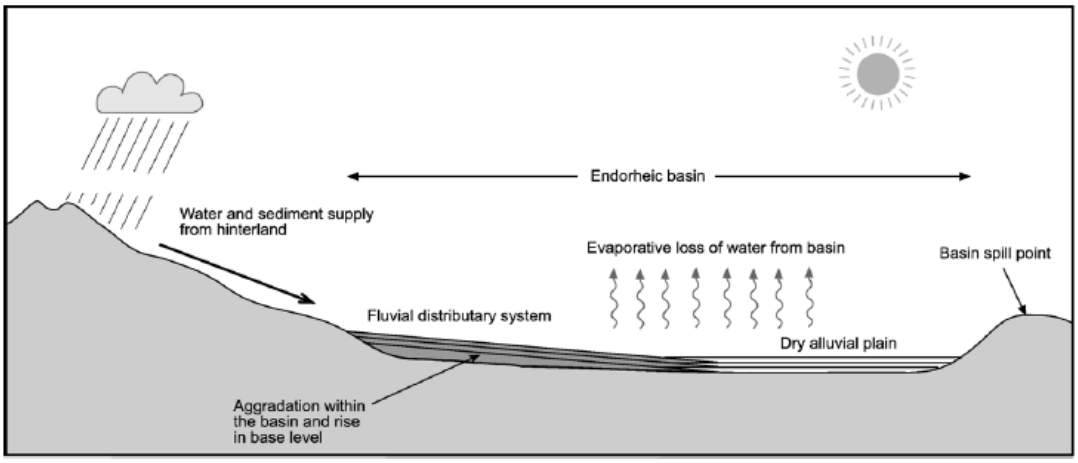

Figure 2. Tectonic and climatic setting for the formation of fluvial distributary systems (Nichols and Fisher, 2007): Due to the evaporation there is a loss of water from the basin, which is one of the factors that make the water lose energy.

As the flow energy is the system is decreasing, the water is less incisive into the subsurface and thereby the size of the channels decrease. As run-off in an arid to semi-arid setting is characterized by short periods of peak water flow, catastrophic overbank flooding's occur during which amalgamated crevasse splays and – at the downstream main-channel end – terminal splays are formed (Donselaar et al, 2013). The resulting morphology at the river system terminus is an intricate pattern of juxtaposed fluvial channels fringed by thin, laterally extensive splay sheets (Donselaar et al, 2013).

Jones and Hajek (2007) describe the floodplain deposits formed during overbank flooding's, as ranging from mudstone to sandstone. They state that the deposits characteristically contain ripple-and dune-scale tabular cross-beds and planar bedding, and typically show evidence of intermittent flow. The floodplain deposits furthermore may exhibit modification by floodplain processes including bioturbation and varying degrees of paleosol development.

An effect of the decline in channel fill sandstones due to the transitions from confined to unconfined flow is, according to Nichols and Fisher (2007), the exponential decrease in the degree of interconnectedness of channel sandstone bodies from the proximal to the distal areas in the Huesca system. However, with the insight of Donselaar et al. (2013), stating that a crevasse contains a distributary network of waning channels that pass into un-channelized flow, it is likely to find a network of sand-filled channels in the distal area of the crevasse splay. As the flow gradually passes into un-channelized flow, it is expected that the sand-filled channels are connected to the sheet floodplain facies.

Torres Carranza (2013) studied the deposition of a modern crevasse splays in Bolivia. His research confirmed the findings of Donselaar et al. (2013). The crevasse splays mapped in his research contain a distributary network of channels with decreasing size in the mapped crevasse-splay deposit.

Torres Carranza (2013) states that the main controlling factor on the grain-size diminution within the crevasse-splay deposits is the increasing distance to a channel (main of crevasse). This phenomenon is explained by the process of dwindling energy of the system. The energy of the system reduces quickly as the flow becomes unconfined and starts waning over the floodplain. At a certain flow rate the water will become unfit to transport coarser sediments and it will only hold fine sediment.

A second phenomena occurring due to the decrease in flow rate is a decrease in layer thickness. The thickness of deposits will decrease away from the channel as floods deposit most of their load near the channel banks (Nichols and Fisher, 2007).

During a field work, two intervals of crevasse-splay deposits in the Huesca fluvial fan are mapped. In order to gain more understanding of the spatial distribution and consequently the depositional mechanisms of crevasse-splays, the field data are processed and analysed. This is done by constructing cross-sections and correlation panel for two outcrop locations of terminating crevasses-splays in the distal area of the fluvial fan. The single crevasse splay layers are studied on geometry, grain size distribution and sedimentary structures, from which the depositional process of one layer can be determined. The crevasse splay intervals are studied on compensational stacking, vertical- and lateral trends and interfering crevasse systems, from which the possible connectivity of the layers is determined.

The result of this study can serve as a basis for conceptual high-resolution static reservoir models of crevasses-splay deposits and may help in developing a predictive workflow for subsurface development of crevasses splay (*tough gas)* reservoirs. Using reservoir analogues as in this study may contribute to get a better insight the uncertainties the in the development of tough gas reservoirs.

This research project is a contribution to the *Tough Gas Proje*ct, performed by the TU Delft.

2. Geological Setting

The Huesca fluvial fan, located in the northern part of Spain, is an asymmetrical radial fluvial fan system in the northern part of the Ebro Basin (Figure 3) (Donselaar and Schmidt, 2005).

The Ebro Basin formed as a foreland basin to the Pyrenean orogenic belt (Figure 4). The Pyrenees developed as a result of crustal shortening between the Eurasian Plate and the Iberian Sub plate during the Pyrenean phase of the Alpine orogeny (Late Cretaceous to Miocene) (Donselaar and Schmidt, 2005; Fisher et al, 2007). The Ebro Basin formed as an autochthonous basin on the Iberian Plate, due to this crustal shortening. Thrust sheets moved southward away from the collision zone between the Iberian Plate en the European plate (Donselaar and Schmidt, 2005). Eroded clastic sediment from the uplifted South Pyrenean Foreland Basin fill provided the sediment source for the fluvial fan (Nichols, 2005).

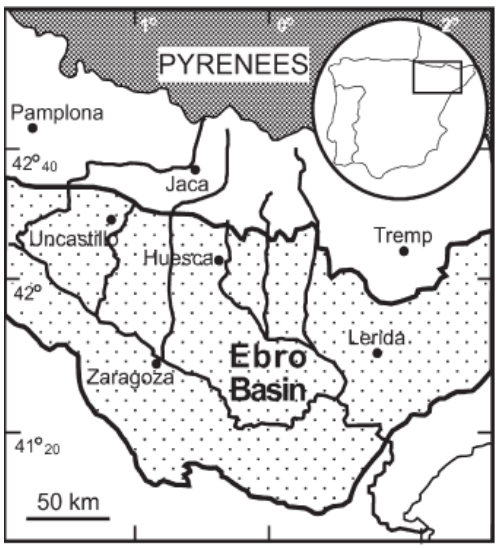

Figure 3. The Pyrenees and the Ebro Basin, the foreland of the Pyrenean mountain belt in the middle to late Tertiary. From Fisher et al (2007).

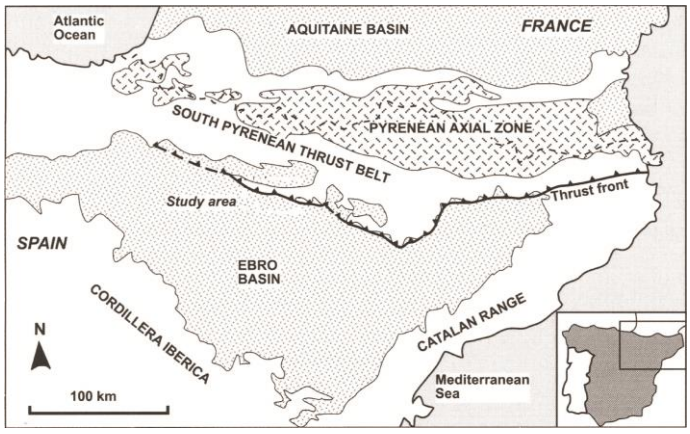

Figure 4. Tectonic and stratigraphic setting of the south Pyrenean thrust belt and the adjacent Ebro foreland Basin, from Nichols (2005).

The southernmost thrust front (Sierras Marginales, Figure 5) was emplaced from Early–Late Eocene (Donselaar and Schmidt, 2005). The thrust front emerged to form a topographic high that separated the Ebro Basin from the South Pyrenean Foreland Basin. Deformation of the Sierras Marginales by the emplacement of a later thrust sheet (Garvarnie thrust sheet) occurred in the Late Eocene and Oligocene and created a 15–20 km wide fractured zone in the Sierras Marginales. This zone forms the line source apex of the Huesca fluvial fan system (Figure 5) (Donselaar and Schmidt, 2005).

The Huesca System has a radius of over 60 km (Fisher et al., 2007). Palaeocurrent data from the fluvial channel deposits show a radial current pattern that has been back-plotted to define a constrained apical region for the Huesca System. However, Fisher et al. (2007) concluded that this apical region is not well constrained for the Huesca system. The main palaeocurrent directions in the Huesca fan change from due south in the proximal part of the fan to southwest and even northwest in the distal part (Jupp et al., 1987).

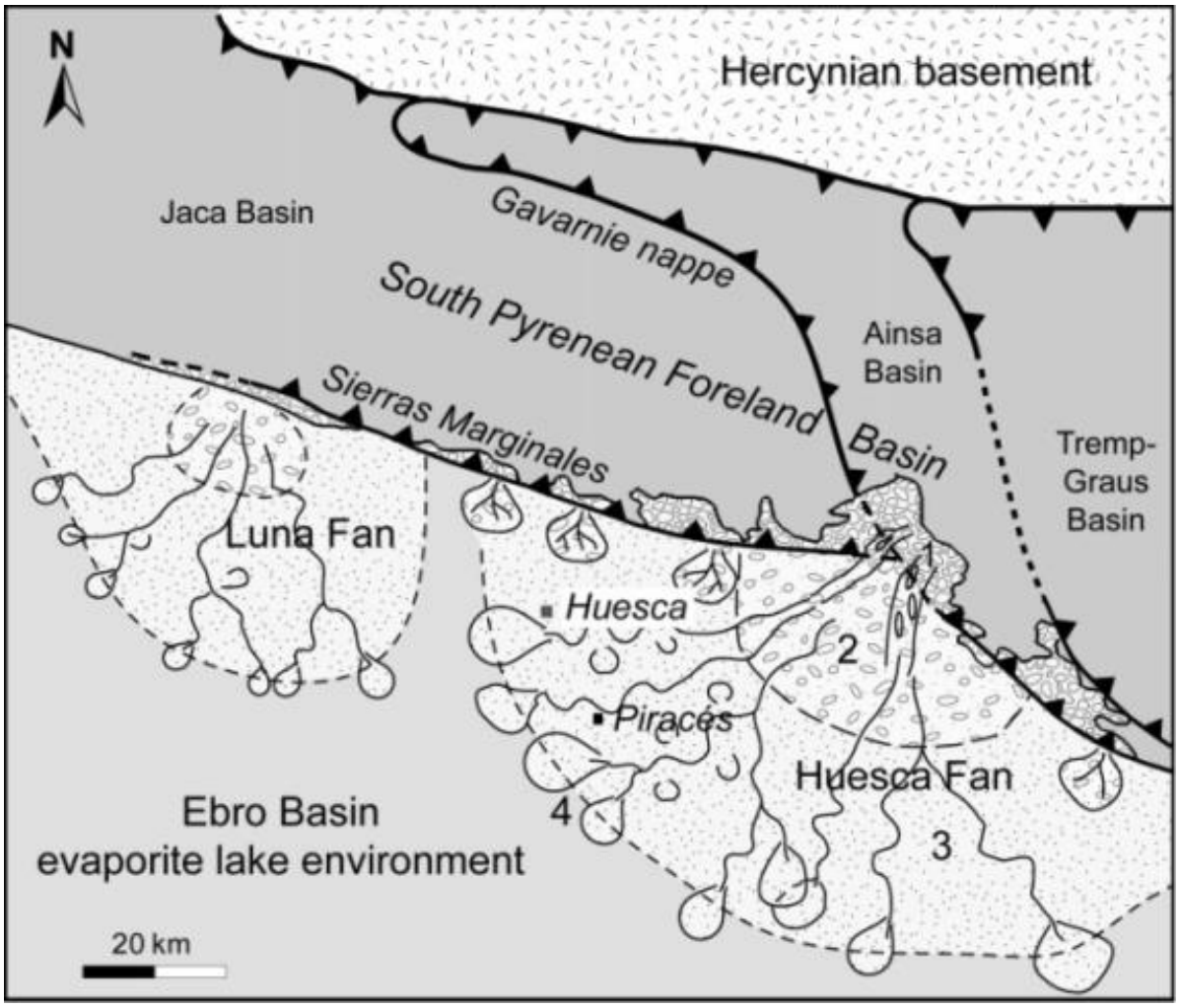

Figure 5. Facies distribution of the Huesca fluvial fan. 1, line source apex with confined conglomerate-filled palaeovalleys in folded and faulted Eocene limestone of the Sierras Marginales; 2, open braid plain; 3, distal fan area with meander belts in a floodplain; 4, fan fringe: small meandering rivers end in terminal lobes and sheets. Huesca: study area of the present paper. From Donselaar and Schmidt (2005)

The Huesca fluvial system shows a decrease in channel depth and grain size distally, as well as an increase in the proportion of sheet sandstones, interpreted as deposits of unconfined flow events (Fisher et al., 2007). The sediment distribution of the Huesca fan shows a general fining grain size from the apex to the fan fringe (Donselaar and Schmidt, 2005).

The fluvial deposits at the fan termination dominantly consist of siltstone and claystone, with interbedded thin, ribbon and sheet-shaped siltstone and very fine sandstone bodies formed by shallow, narrow meandering streams (Donselaar and Schmidt, 2005).

3. Data and Methods

A two-weeks-during field work is performed in April 2014 to gather data of the crevasse splays in the distal area of the Huesca fluvial fan. These crevasse splays are a good analogue to the Triassic, Rötliegend and Bundsandstein intervals in the West Netherlands Basin.

3.1 Outcrop description

The study area lays approximately three kilometres North West of Huesca (Figure 6). The fan deposition is exposed here as thick siltstone and claystone succession, with some fluvial sandstone bodies. Two specific outcrop locations were studied: (1) the dam 'Embalse de Montearagon', and (2) an outcrop location 1.5 kilometres northwest of the town of Quicena. At the dam a section of about 550 m wide and 60 m high is exposed. The outcrop has a vegetation overgrowth of about 5 percent and a cliff steepness of about 25 percent. At the Quicena outcrop location, the study area exists of four coves, mainly covered by vegetation. Preliminary results from GPS measurements suggest that the two outcrops lie within the same stratigraphical interval (Figure 7), with a spacing of approximately one kilometre.

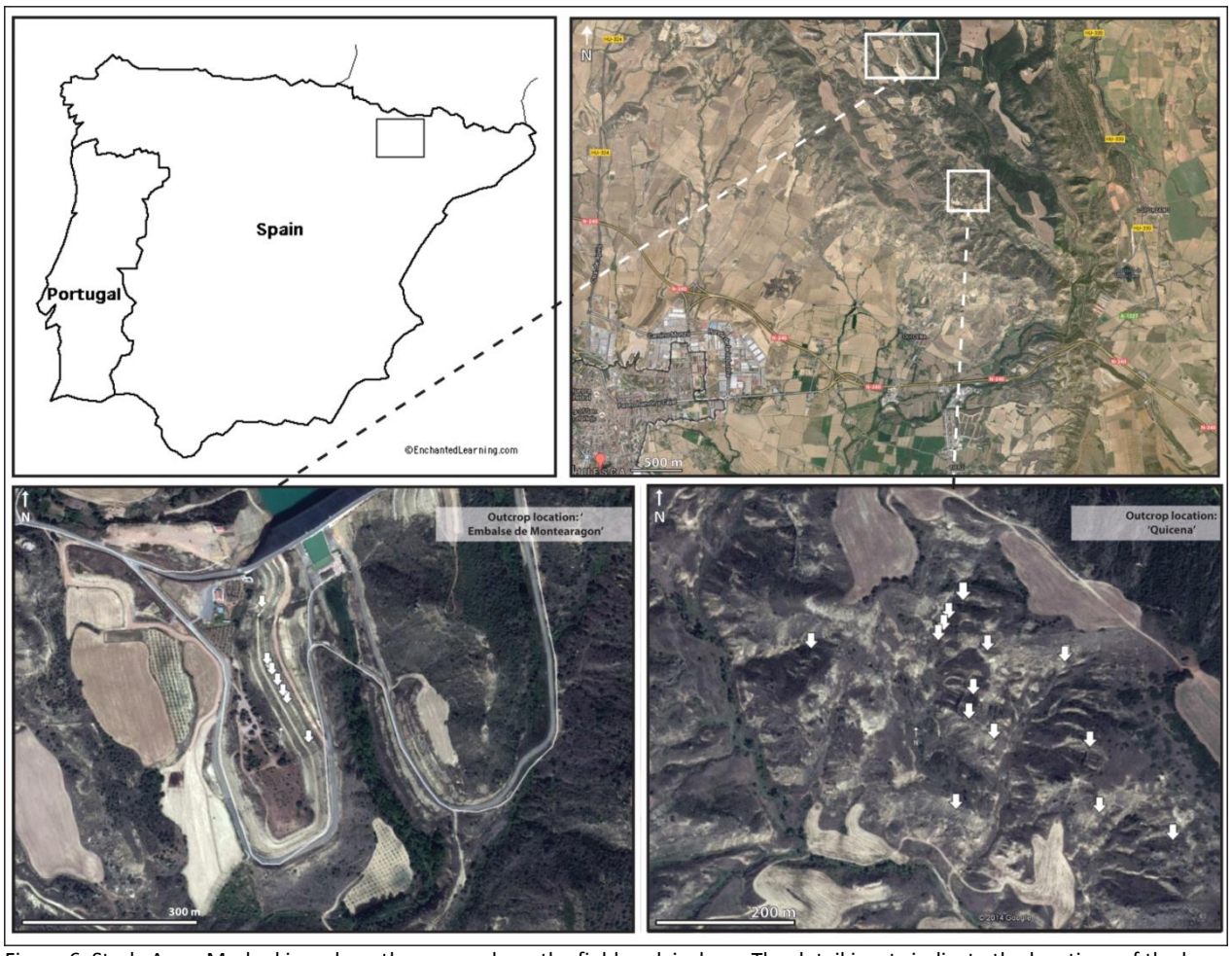

Figure 6. Study Area. Marked in red are the areas where the fieldwork is done. The detail insets indicate the locations of the logs with the green and blue pawns. A larger version of these maps can be found in Appendix C

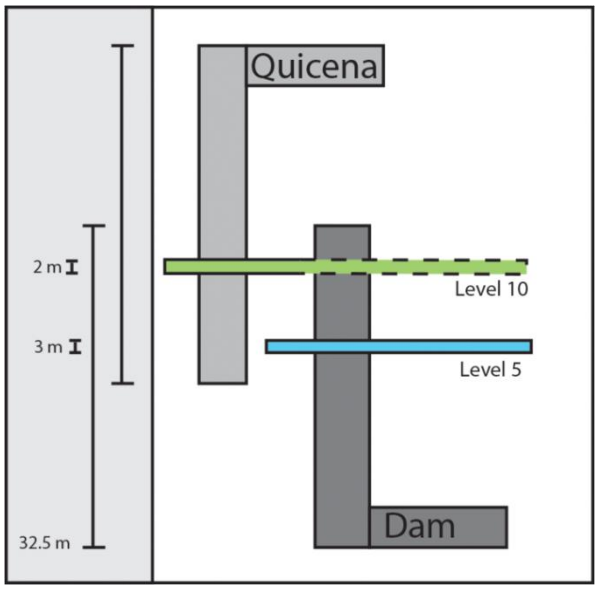

Figure 7. A schematic overview of the sedimentary correlation between the two outcrop locations and the selected intervals.

3.2 Data acquisition

At the two outcrop locations an interval of crevasse-splay deposits is mapped, using a type section log, detailed lithostratigraphical logs, photo-panels and lateral characterizations of sand beds.

Type-sections are made for both outcrop locations, which are then correlated using dGPS measurements. The structural dip is reconstructed by triangulating the top of a distinctive pinkish to dark red-coloured paleosol layer in the Quicena outcrop (Figure 8). The resulting structural dip is combined with the absolute altitudes of reference points within the type sections to arrive at a solid correlation.

A selection of two sedimentary intervals is made on the basis of the type-section log (Figure 7). At several places along the outcrops (Figure 6) detailed logs of the selected intervals are made, neglecting the small structural dip. The logs along the fluvial succession are two-to-three meters in length. All log locations are geo-referenced, partly with a handheld Garmin 62stc GPS meter (horizontal accuracy of three to five meter), and partly with a Trimble R7 dGPS meter (accuracy of cm to dm).

Furthermore, three photo-panels are made in the field. One is made at the dam outcrop location of the total exposure of the North East side of the dam, and two are made at the Quicena outcrop location. With these photo-panels a lateral characterization of the sand beds is made by recording the grain size distribution, thickness, bed boundary definitions and the flow directions in the field along the photo-panels. The photo-panels are also used for in-field correlation of the detailed lithostratigraphical logs.

Figure 8. Distinctive pinkish to dark red-coloured paleosol layer in the Quicena outcrop used to reconstruct the structural dip

3.3 Data processing

The main flow direction at the study area was determined by earlier studies (Figure 9, Nichols and Hirst, 1998). The southeast to northwest flow direction indicates that the Quicena outcrop lies more proximal then the Dam outcrop.

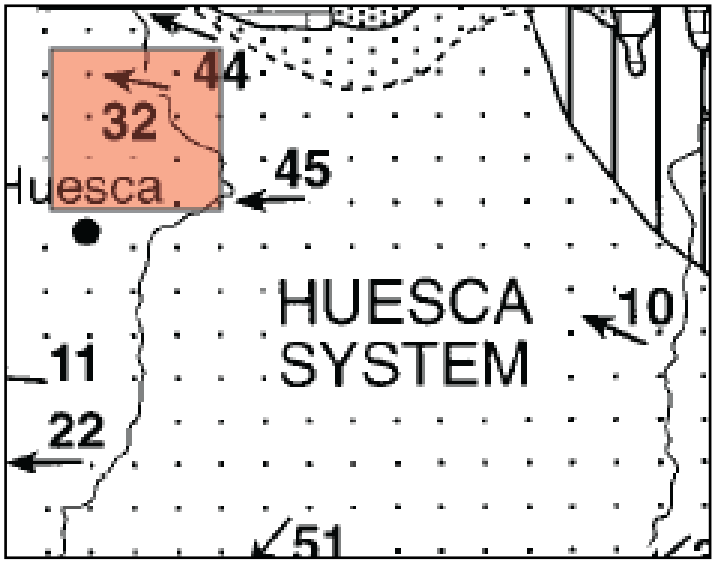

Figure 9. Paleoflow directions. The number of readings in each area is indicated adjacent to arrows showing mean trends. The red square is the studies area. (Edited from Nichols and Hirst, 1998)

Based on the photo panel at the dam, a correlation panel is constructed. This is done by projecting closely spaced sedimentary log sections onto the photo panel with the help of the corresponding GPS data. The visible layer boundaries are mapped, the remaining layer boundaries are determined by

interpolation. The N-S orientation of the outcrop coincides with the axial cross-section through the crevasse system, where south is more proximal then north.

Due to the irregular positioning of outcrops along the coves at the Quicena outcrop, it is not possible to make a linear correlation panel of this section. To gain more insight in the three-dimensional distribution of the grain-size and layer-thickness distribution, seven cross sections through the logs are defined (Figure 10). Five sections are parallel or perpendicular to the main flow direction, and two cross-sections have an angle of about 45 degrees to the main flow direction of the crevasse splay. The detailed lithostratigraphical logs are projected onto the cross-sections and combined with photo-panel interpretations to correlate and characterize the individual thin-bedded sand sheets.

To gain insight in the grain-size distribution, grain sizes recorded in the detailed logs are projected onto the cross sections and interpolated in a schematic overview. In section Q10-1 to Q10-4 additional grain size data from the photo correlation panel is used to verify the interpolated overview.

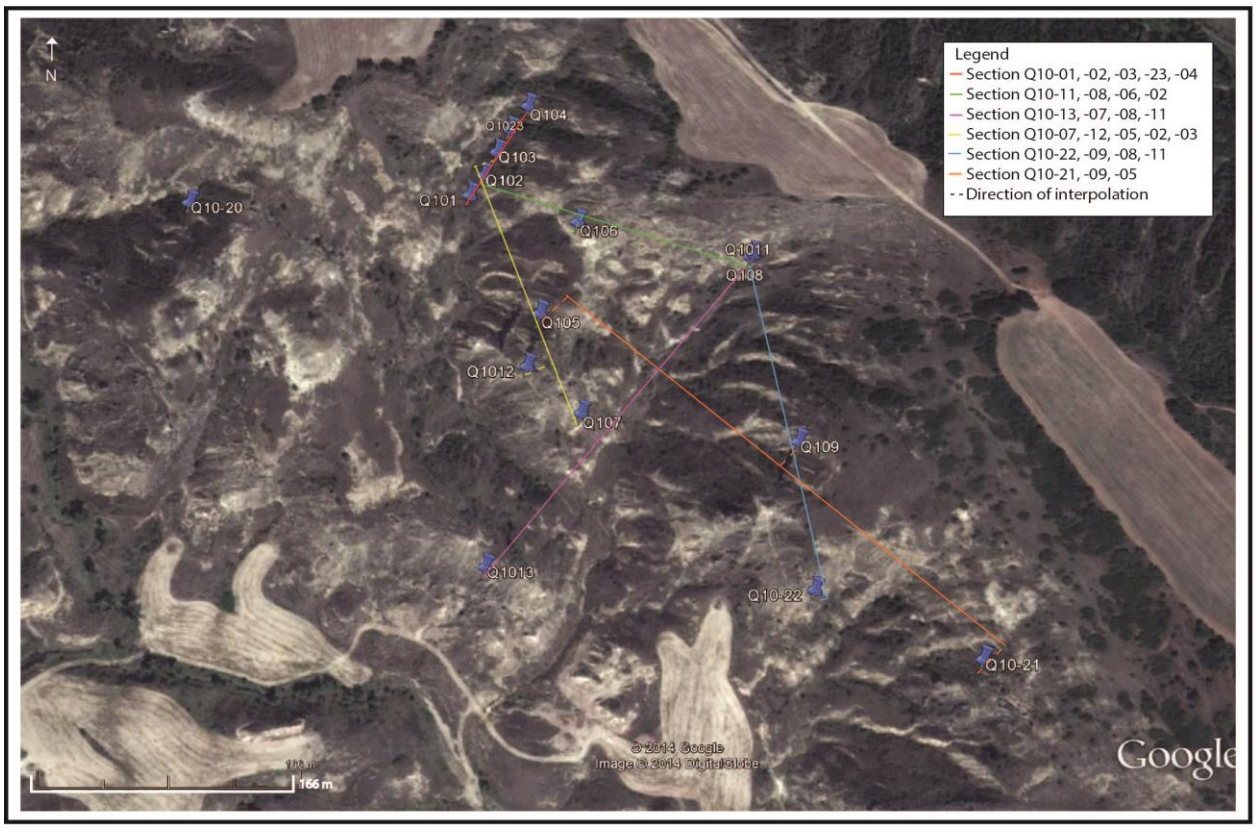

Figure 10. Log locations at the Quicena outcrop and cross-sections through the log locations.

4. Results

Two sedimentary intervals are studied in detail, named level 5 (L5) and level 10 (L10 or Q10). Level 5 is only found at the dam outcrop (Figure 7). Level 10 is best exposed in the Quicena outcrop, but is probably also encountered in the Dam outcrop.

Level 5 is an exposed over the total width of the dam outcrop (550m) with an average interval of 3m and seems to be thinning proximal to distal. The layer boundaries are harder to detect in the distal area.

Level 10 is most profound at the Quicena outcrop, here it is exposed as a 2-2,5m thick interval. When correlating this level to the dam outcrop a probable continuation of this level is encountered, however with a significantly smaller thickness. Level 10 exposes more fluctuation in thickness then Level 5.

4.1 Lithofacies types

4.1.1 Floodplain fines

Floodplain fines can be found as laterally extensive sheets (550 m at the dam, Figure 12) with grain sizes ranging from silt to clay. The floodplain deposits are overall deeply weathered, sometimes coloured from grey into ocher or red.

4.1.2 Crevasse-splay deposits

Crevasse deposits have a grain size ranging from sand to silt and are also laterally extensive sheets (550 m at the dam, Figure 12). Some layers contain a highly bioturbated blue-grey top and an incising, locally undulating, base. A variety of sedimentary structures can be found in the sheets: tabular cross-bedding, through cross-bedding, current ripple lamination and amalgamation surfaces.

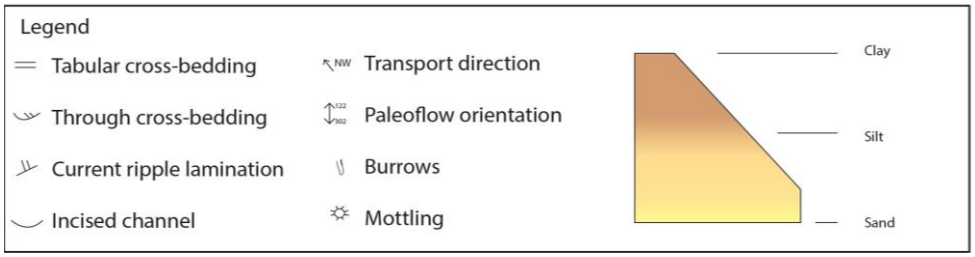

Figure 11. Legend of the symbols and colours used in the logs and the correlation and cross-section panels

Figure 12. Correlation panel of the dam Outcrop. On the correlation panel the found boundary layers and a grain size distribution are displayed. Note that vertical aspect ratio is not corrected.

4.2 Sedimentary features

4.2.1 Stacked crevasse splays

The stacking of the individual layers comprises an accumulation of floodplain fines and crevasse deposits. Crevasse deposits are often found in stacks up to two meters in thickness (Figure 13).In both level 5 and level 10 there is an increasing in flow energy in the stack (Figure 13). The increasing number of erosional and undulating surfaces from bottom to top indicates an increasing energy of flow per depositional event.

Proximal stacking of crevasse-splay deposits contains sand-on-sand contacts, due to the erosional boundaries and amalgamation surfaces (Figure 13). Due to the higher flow energy near the crevasse-splay apex, the deposited grain sizes range from very fine sand to silt. The smaller grain sizes (mainly silt) are eroded, due to the erosional boundaries and amalgamation surfaces.

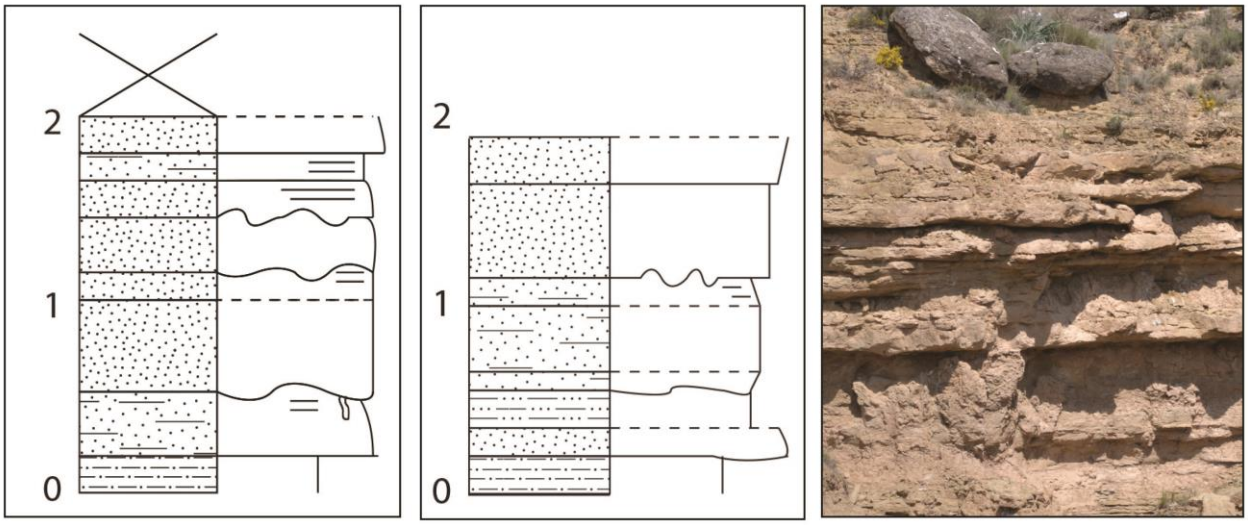

Figure 13. Stacks of crevasse-splay deposits (Log Q101, log Q102 and picture). A stack can be up to two meters in thickness. The flow energy is increasing from the bottom to the top of the logs, picture is illustrating this same characteristics.

The interval of stacked crevasses is thinning in a distal direction (Figure 14). The apparent thinning to thickening in the first 300 m of the Dam outcrop is caused by the non-axial cut through the crevasse splays (Figure 12). It can be concluded that the wedge shape that Torres Carranza (2013) found for a single crevasse-splay layer (Figure 15), can also be found in intervals of stacked crevasse splays. Distally, the stacking fluctuates more in thickness (Figure 16). The thickness of the stacked interval varies from 1.5 to 1.75 meters; this gives a fluctuation of 17%. Despite the abundant fluctuations in general, the cross-section perpendicular to the main flow direction corresponds with the half of the lens shaped that Torres Carranza (Figure 15) describes.

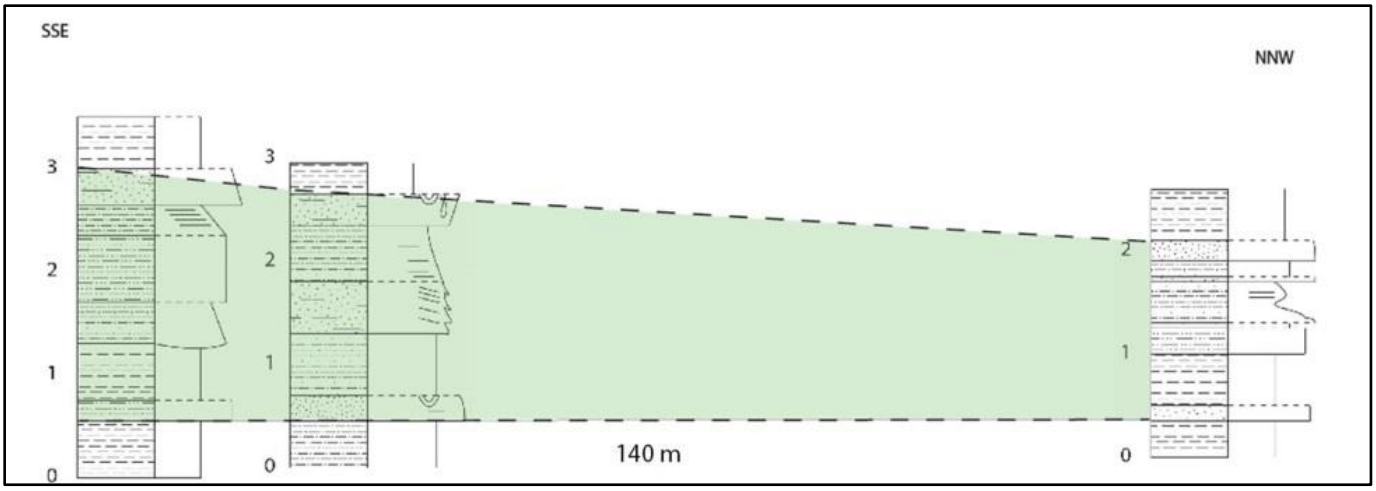

Figure 14. Proximal to distal thinning of a stack of crevasse-splay deposits.

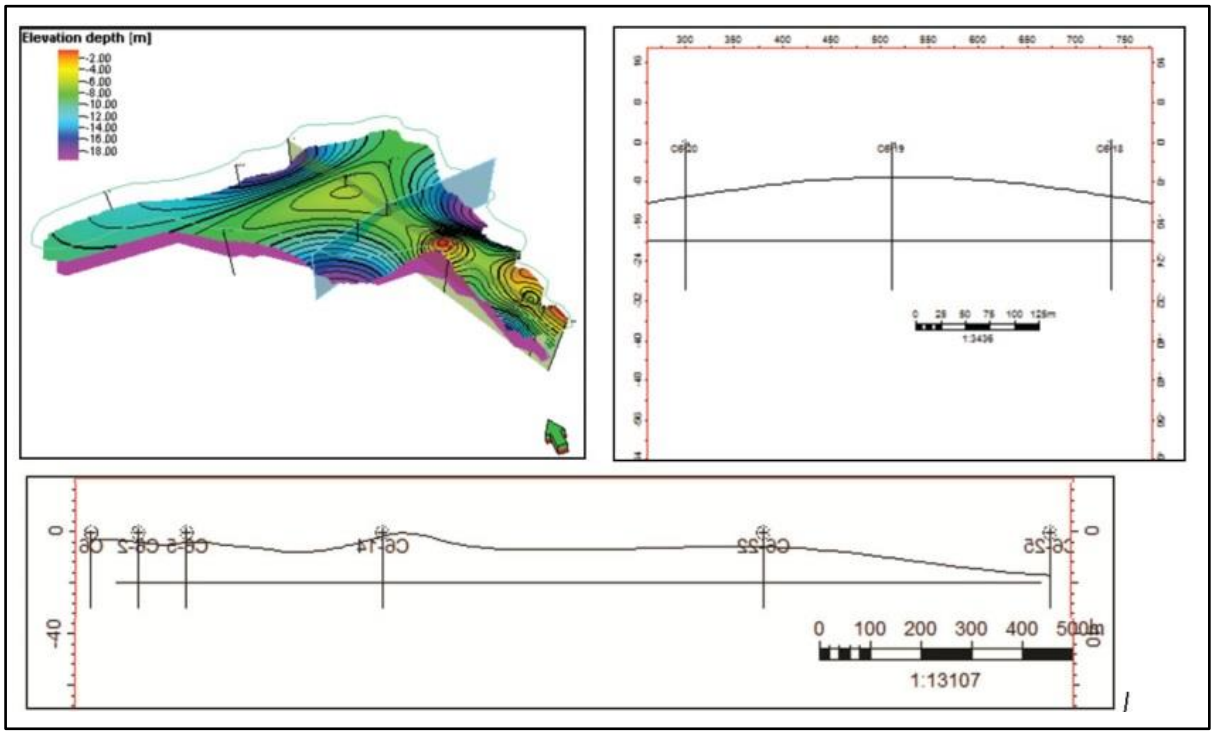

Figure 15. Thickness distribution in a crevasse-splay deposit (edited from Torres Carranza, 2013)

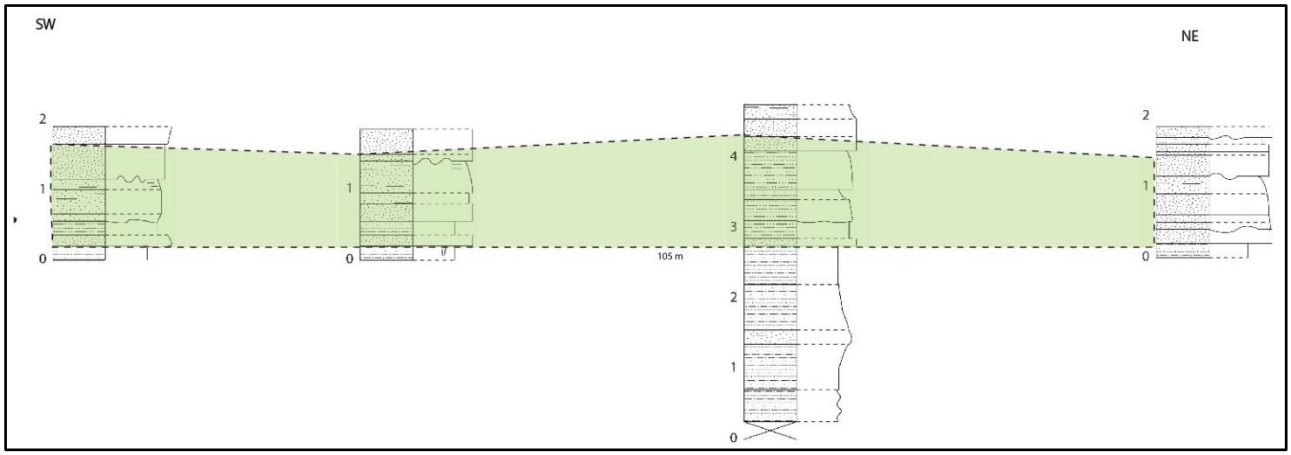

Figure 16. Cross-section perpendicular to the main flow direction, showing the fluctuating thickness of a stack of crevasse-splay deposits

The stacked crevasses continue laterally over 550 meters. The sandstone stack at the dam is composed of several layers. Moving from proximal to distal, the sandstone stack composed of five layers (L512, Figure 17) separates into a stack of seven layers (L511), with individual thicknesses of 10-30 cm. The interfering layers can be explained by two processes (1) the silt or clay sheets are eroded proximally by the higher flow energy and (2) layers from a different crevasse complex are interfingered.

Distally, the number of layers further increases (Figure 18). The most logical option here is that the incoming layers are an interfingering crevasse system. The flow energy is not strong enough here to incise into previous crevasse deposits.

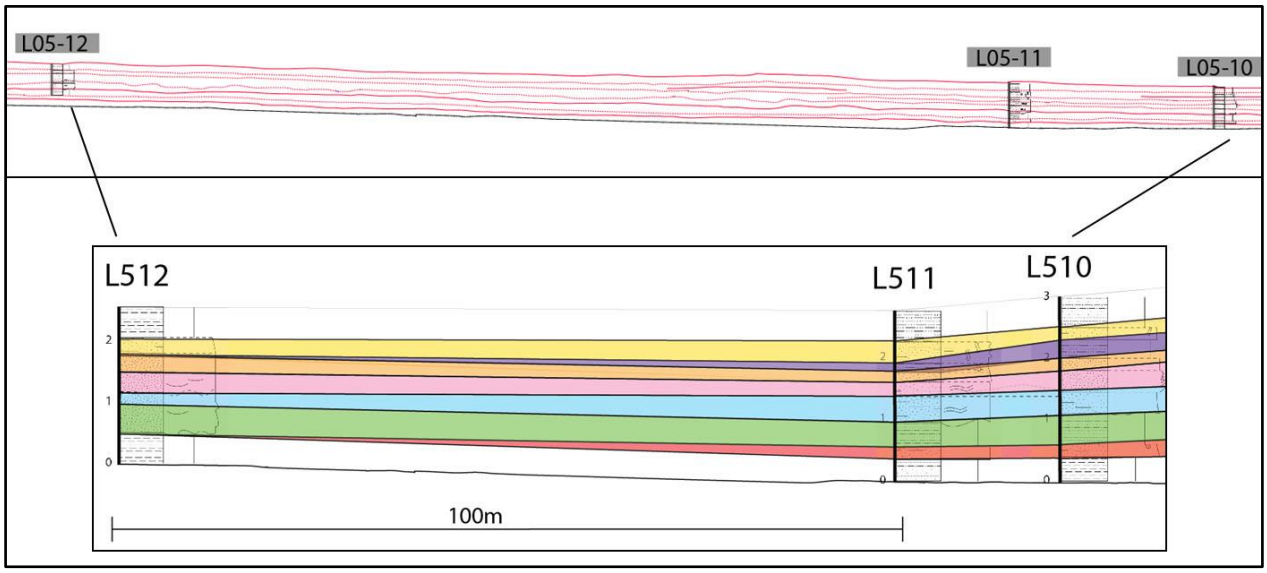

Figure 17. (1) Correlation panel and (2) Schematic display of the correlated layers at the Dam outcrop. This section is located proximally.

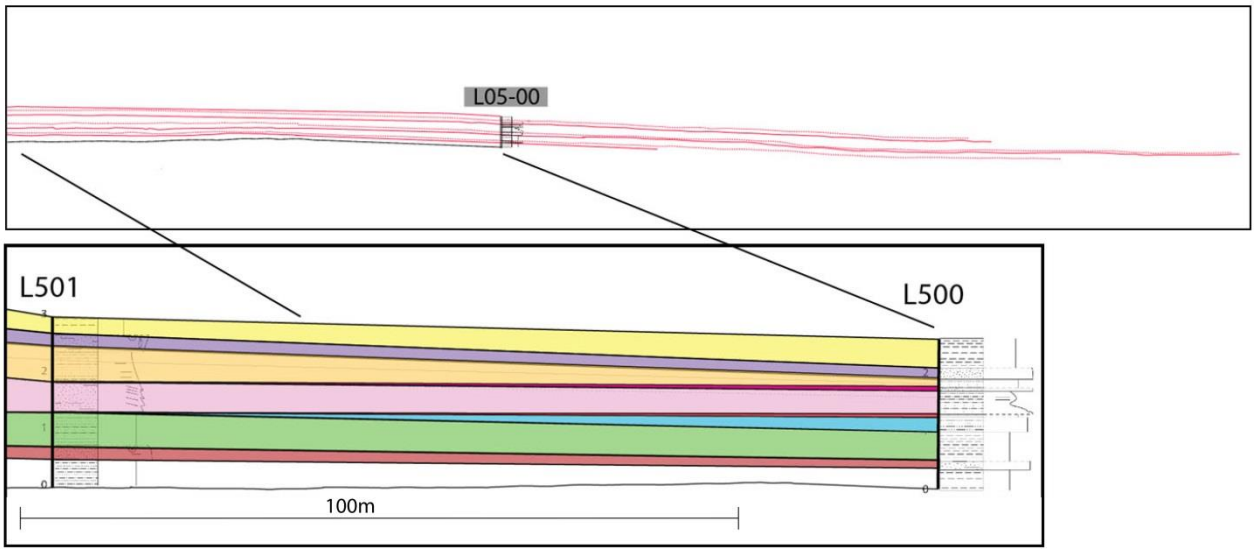

Figure 18. (1) Correlation panel and (2) Schematic display of the correlated layers at the Dam outcrop. This section is located distally,

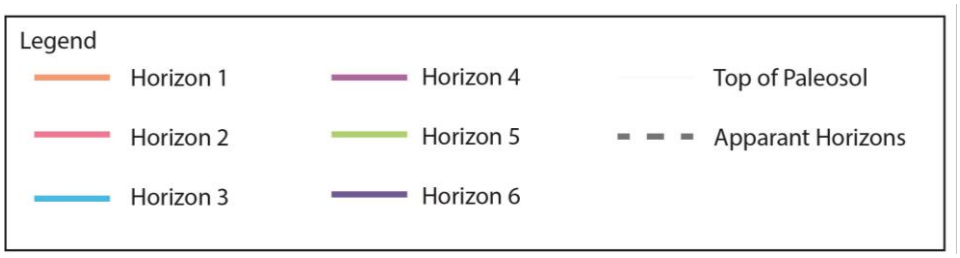

Figure 19. Legend of the horizons in the Log correlation cross-sections.

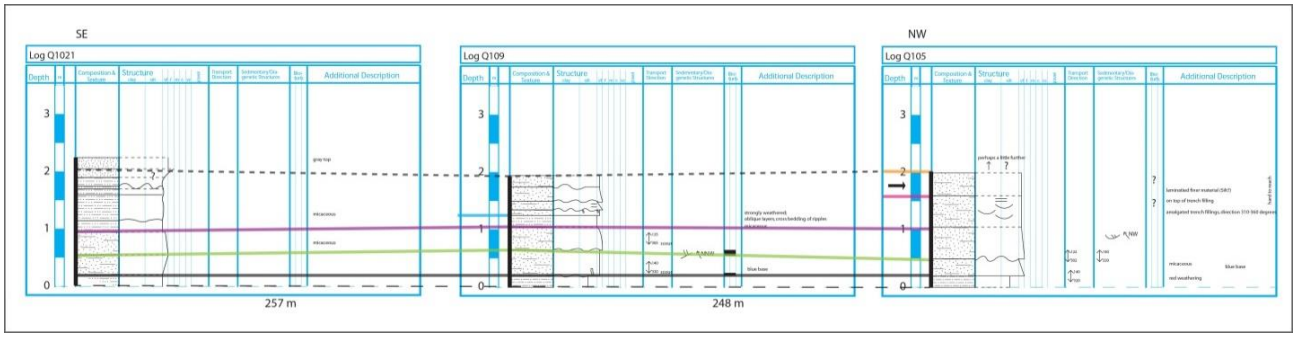

Figure 20. Correlation cross section of Log Q1021, Q109 and Q105. The top layers of the interval cannot be linked.

4.2.2 Single crevasse splay

The individual layers vary in thickness from 5 to 60 centimetres. Looking from proximal to distal, a wedge shape can be found (Figure 21), which confirms the finding of Torres Carranza (Figure 15). The layer thickness decreases with increasing distance to crevasse-splay apex. Proximally, it is harder to determine general trends due to the thickness fluctuations (with a maximum of 40 centimetres) (Figure 22).

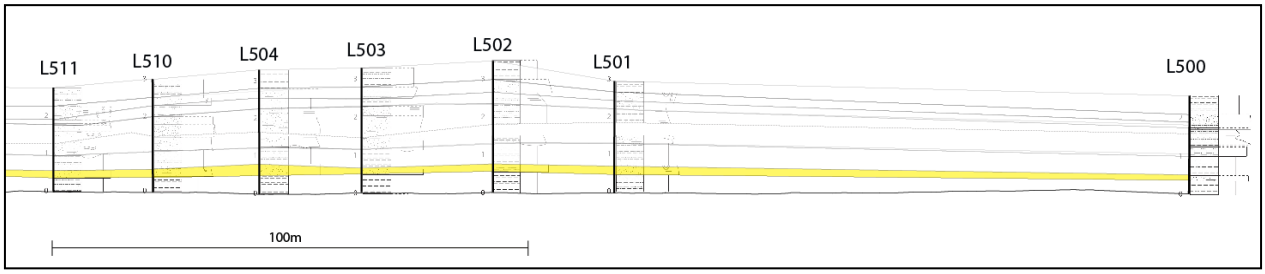

Figure 21. Thinning of a crevasse splay from proximal to distal.

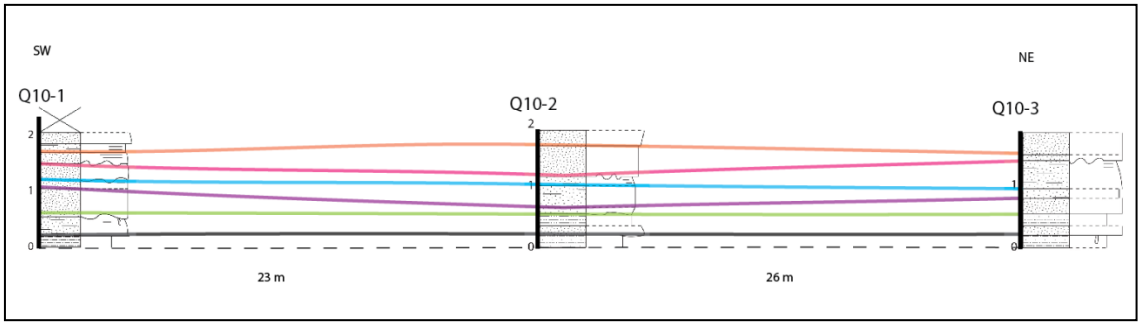

Figure 22. Thickness fluctuations of proximally located crevasse splays.

Moving from proximal to distal, the boundaries become less undulating and incisive as the flow energy is decreasing (Figure 23). Proximally, low contrast in grain sizes locally obscures the boundaries of amalgamated layers (Figure 24). Distally, the grain size of the crevasse splays conforms to the grain size of the floodplain fines, also making layer boundaries hard to detect.

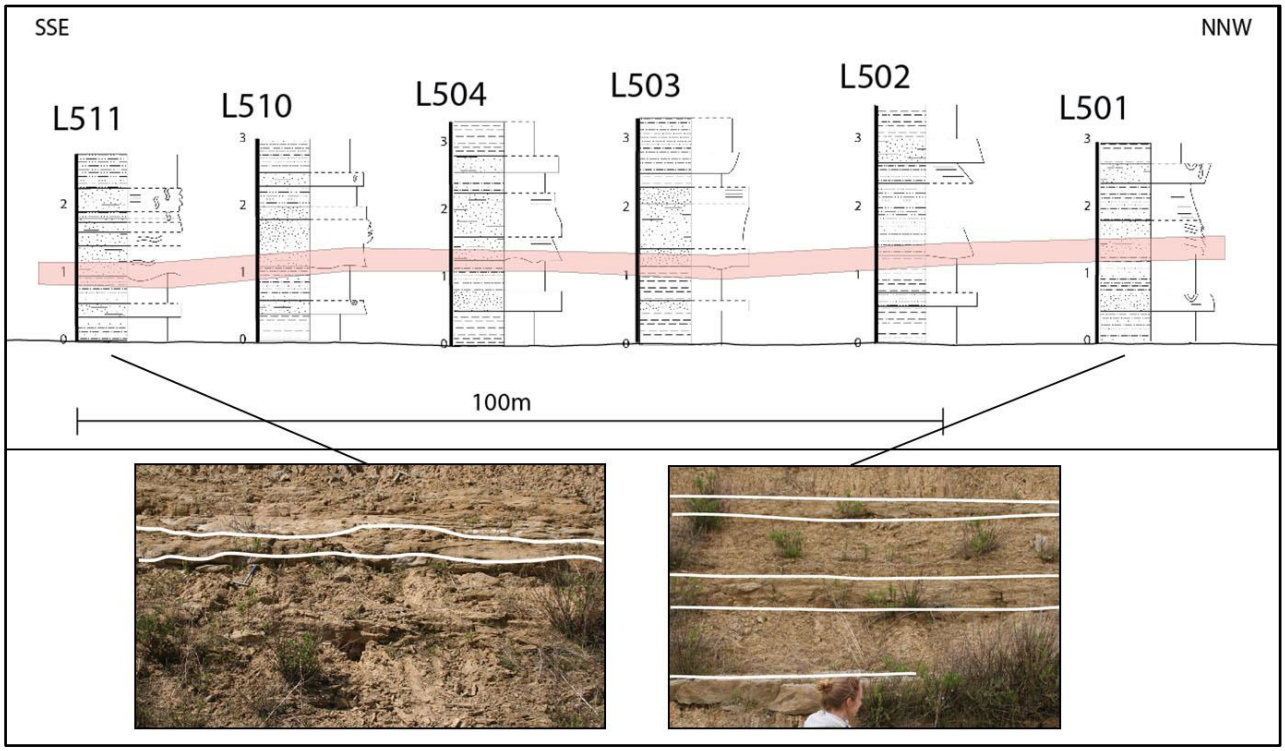

Figure 23. From proximal to distal, the boundaries become less undulating and incisive as the flow energy is decreasing.

Most sedimentary structures are found in the sandy crevasse-splay deposits. Proximally, trough cross-bedding and current-ripple lamination are encountered. All layers contain traces of bioturbation, often throughout the entire layer (Figure 24). Moving to the distal area, the amount of horizontal laminations increases, and the bioturbation is limited to the sandiest layers (Log L501, Figure 24). Furthermore, there are traces of burrows which are mainly found in layers that are overlain by floodplain deposits or silty crevasse-splay deposits (Figure 24).

The floodplain deposits are generally deeply weathered, containing coloured bands ranging from ocher or red. The deep weathering makes it impossible to detect sedimentary structures in the floodplain deposits.

The crevasse-splay deposits often contain a highly bioturbated blue-grey top (Figure 24), this is indicative for a submerged environment in which the supply of oxygen is insufficient for oxidisation.

The flow direction is determined by the encountered sedimentary structures (Figure 24). The measured paleoflow directions, recorded in the detailed logs, confirm the southeast to northwest flow direction found in literature (Nichols and Hirst, 1998). Channel incisions, ripples and trough cross bedding indicate the direction of flow at the moment of deposition or directly after deposition.

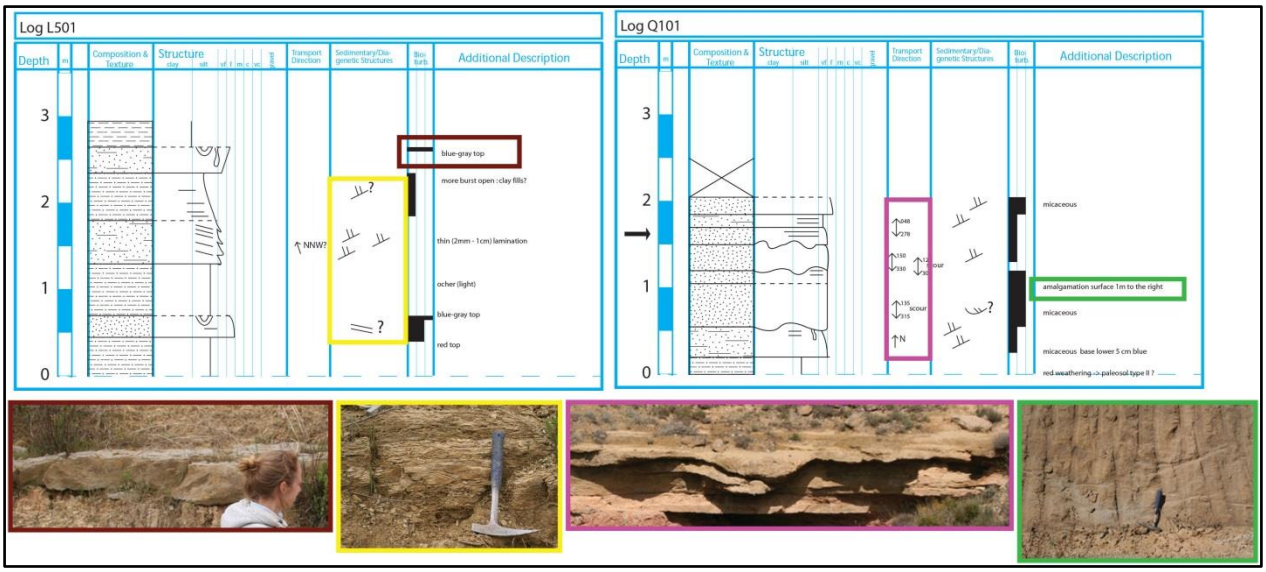

Figure 24. Examples of the mapped sedimentary structures.

4.2.3 Grain size trends

In the grain-size trends, a distinction between proximal and distal behaviour can be made.

A high degree of heterogeneity is found proximally, where there is an internal fluctuation in grain size in the layers (Figure 25). The grain size gradually changes from sand to silt and then back to sand. The observation made by Torres Carranza (2013, Figure 26 and Figure 27) that the proximal heterogeneity is caused by the presence of distributary crevasse channels is confirmed.

The grain size gradually changes from proximal to distal. The main grain size of de the sediments at the left side of the panel is sand, which indicates a higher flow energy (Figure 28). This is in agreement with the determined direction of crevasse build-out.

Within 200 m from log L512 (Figure 28), the dominant grain size changes from sand to silt. Fining-upward sequences within the single layers are mainly found in the distal area.

The observation that the conditions under which clay is deposited can be related to the waning processes and the effect of the deceleration of the flow is confirmed by Banerjee (1977) and Torres Carranza (2013).

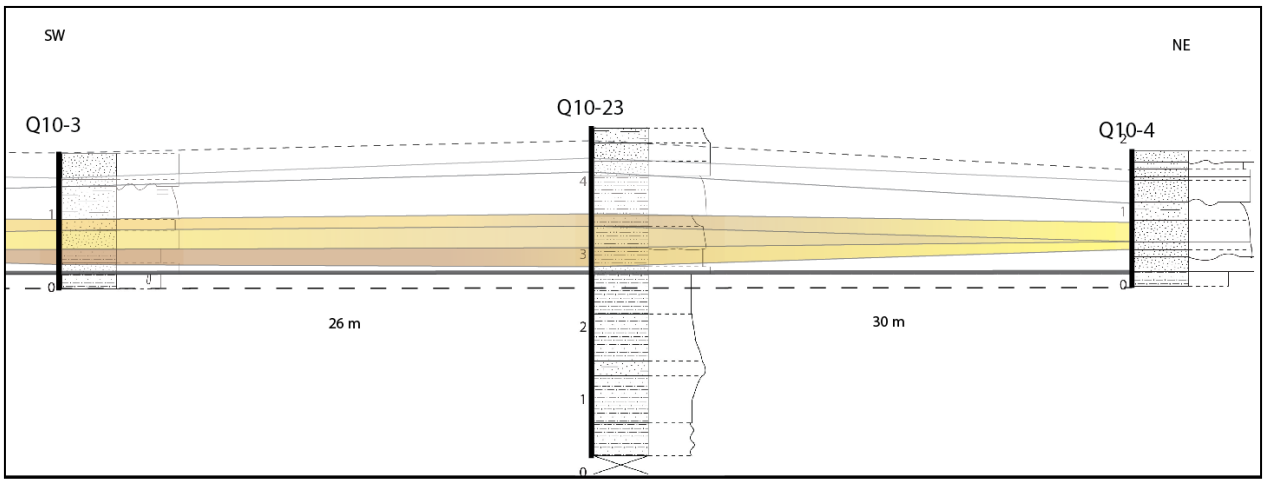

Figure 25. Proximal grain size distribution. Cross-section of perpendicular to the main flow direction/

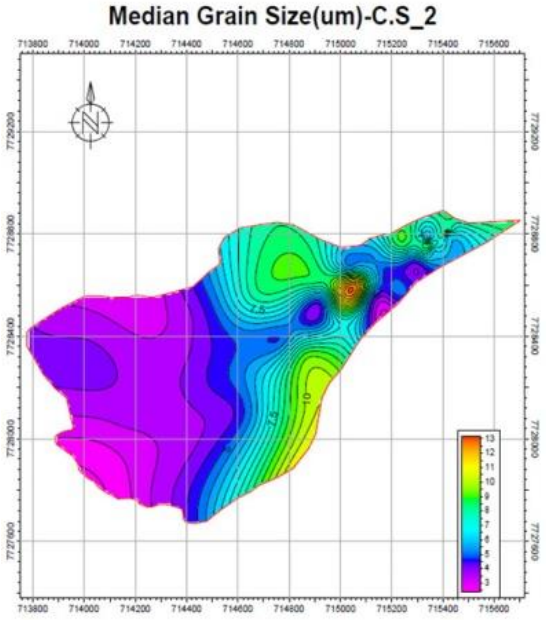

Figure 26. Median grain-size distribution in a crevasse splay (Torres Carranza, 2013)

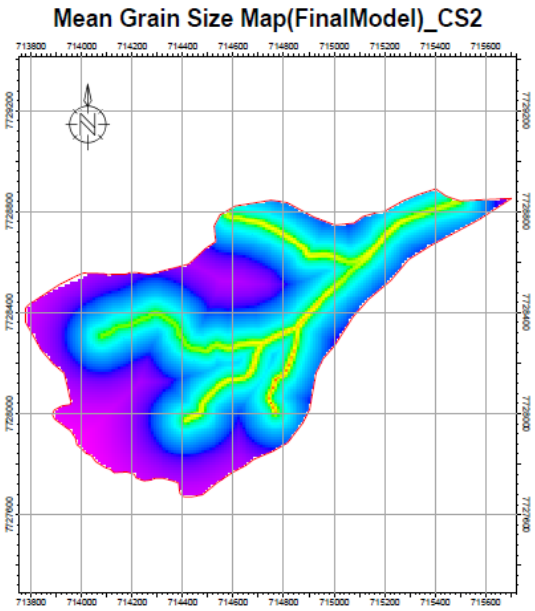

Figure 27. Mean grain size distribution model, for a crevasse splay. The dependence of the grain size distribution to the crevasse channel can be seen (Torres Carranza, 2013).

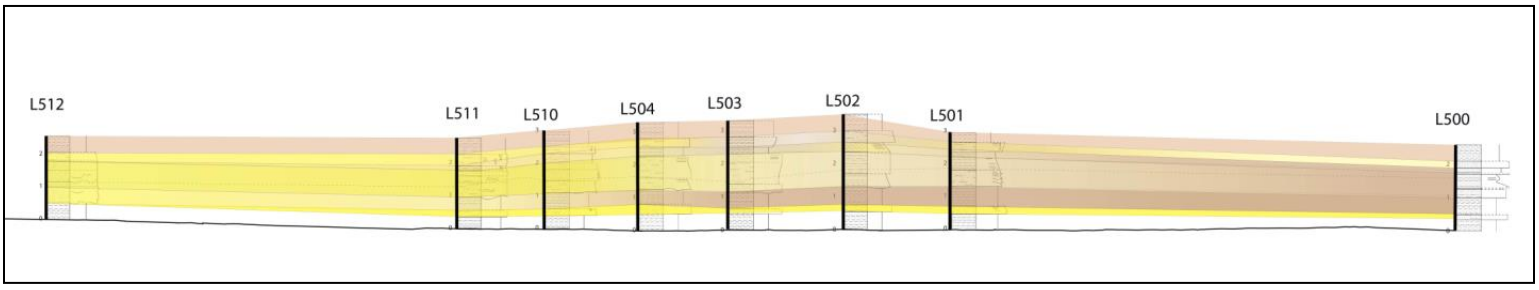

Figure 28. Grain-size distribution from proximal to distal, along the main flow direction.

5. Discussion

The found results can be used to determine the potential for crevasse splays as an hydrocarbon reservoir.

Single crevasse splays display a general decrease in grain size from proximal to distal, where the variation in grain size is higher in the proximal area and probably related to the proximity of distributary channels within the crevasse splay. Distributary channels cut into the underlying crevasse and thus create sand-on-sand contact, effectively connecting the single crevasse splays (Figure 29.).

Grain size is directly related to porosity: as the grain size increases, the porosity is increasing. Hence it is expected that porosity is higher in the proximal areas, where the grain size is coarser, then in the distal areas. As permeability is also a function of the grain size, the same is expected for the permeability distribution. The sand-on-sand contact in the proximal areas results in a large connected volume of multiple crevasses.

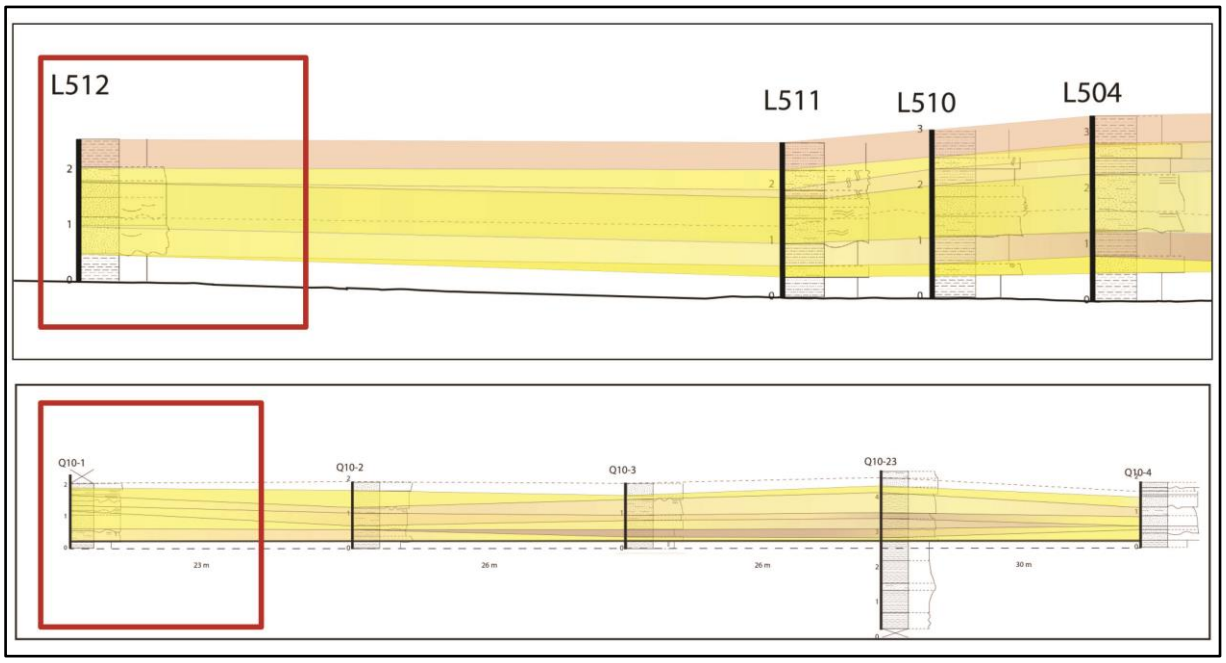

Figure 29. Stack of sandstone layers. Due to a combination of amalgamation surfaces and incising surfaces sand-on-sand contacts are created.

A stacked interval of minimal 50 centimetres can be found over the entire Quicena outcrop in level 10 (Figure 30). The accumulation of log locations accumulates an area of approximately 500 000 m2 (Figure 31). With this dimensions a Bulk Rock volume of 70 000 m^3 is found.

With a few assumptions made (porosity, N/G, water saturation and pressure and temperature characteristics, appendix G), this leads to a STGIIP of 53 * 10^6 cu.f.

Level 10 probably continuous to the dam outcrop (Figure 7). With these assumptions a second calculation can be done. If the 50-centimeres stacked interval continuous to the dam (Figure 32), a Bulk Rock Volume of approximately 400 000 m^3 is found and an associated STGIIP of 307 10^6 cu.f. This is a conservative approximation; when the crevasse really continuous to the dam, it is expected to find a fan shaped body, and thus the depositional area is expected to be significantly larger. The calculated STGIIP gives an indication of the possibilities of these crevasse-splay deposits as a hydrocarbon reservoir.

Figure 30. Continuation of three layers of level 10 over the total outcrop length.

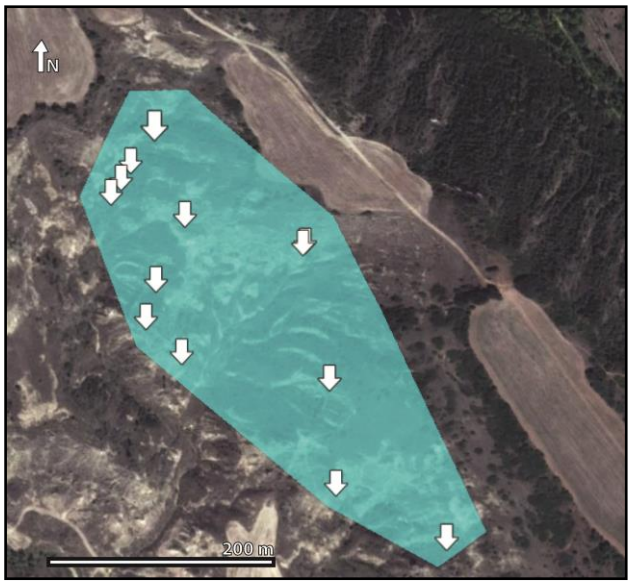

Figure 31. Depositional area of a crevasse splay. A stacking of minimal 50 centimetres can be correlated over the blue area.

Figure 32. Potential depositional area of a crevasse splay, based on the potential correlation of level 10 from the Quicena outcrop to the Dam outcrop.

The depositional settings in the distal areas of the studied Huesca fluvial fan (Miocene) of the Ebro basin in Spain are a good analogue to the Permian Rötliegend and Triassic Bundsandstein intervals in the West Netherlands Basin. The semi-arid conditions in an endorheic basis and the low gradient lower coastal plain are corresponding characteristics of the depositional environments of all intervals. The characteristic sequence of crevasse splays determined in the field can be detected in cores of the intervals in the West Netherlands Basin (Figure 33).

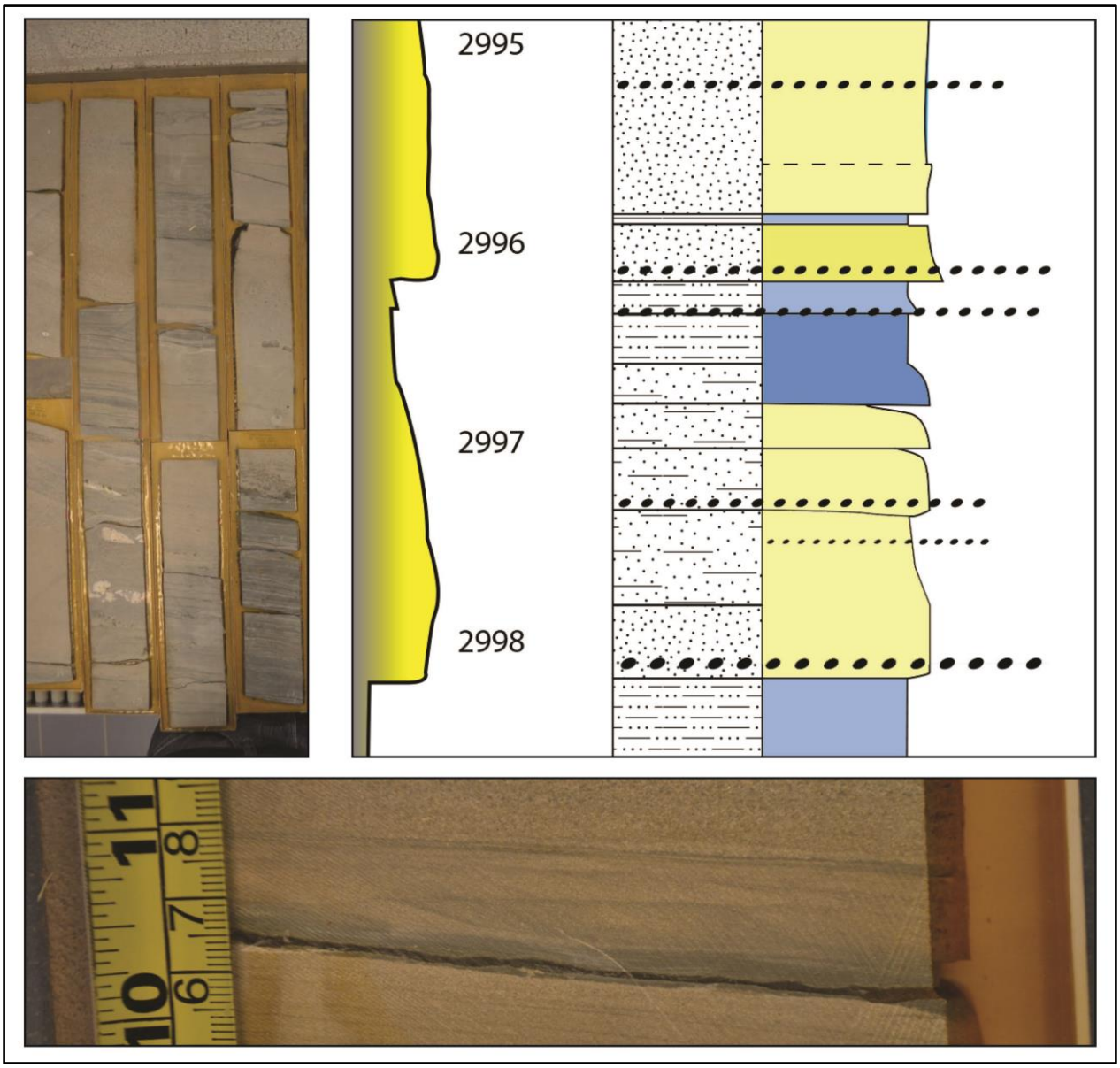

Figure 33. Core from the Triassic interval in the Pernis West-1 well. The characteristic sequence of crevasse splays determined in the field can be recognised in the stratigraphical log made of the logs.

7. Conclusions and recommendations

7.1. Conclusions

The crevasse splay is formed by a combination of channelized flow (incisive thick sandstone layers) and un-channelized flow (mud and sand sheets). The study showed that more proximal to a crevasse channel, the incising flow will remove the smaller grain sizes at the upper part of the layer, and mainly sand will be deposited due to the higher flow energy. This will fade out the contrast between the layers.

The layer thickness will decrease with increasing distance to the main and crevasse channels. More proximal: the layers fluctuate more in thickness then at the Dam, a distributary network of crevasse channels can be found. It can be concluded that that the heterogeneity in the deposition decreases proximal to distal. Crevasse channels are an important feature that controls the depositional processes.

One could see that the crevasse channels have a preferable depositional area, steered by incisions of previous crevasse channels. The first major flooding events will create a preferable path for the next flooding events.

In defining the reservoir potential, it is important to take into account that the highest porosity can be found in the network of distributary channels. The proximal sand-on-sand contact, resulting from the incision of crevasse-splay channels into underlying sand beds, yields a large connected volume of multiple crevasse splays.

7.2 Recommendations

With this research, an additional step is made in the study of the reservoir architecture of crevasse-splay deposits. However, there still is more research needed in order to get a full insight in the depositional processes en the reservoir possibilities of crevasse-splay deposits.

The possibility of building a three-dimensional model with interpolated surfaces must be investigated to gain a better insight in the three-dimensional distribution of the layer thickness and the grain-size distribution. Understanding the grain-size distribution of the individual crevasse channels is necessary to improve the model.

Furthermore, it is recommended to correlate more logs in the field instead of during the desktop work. This will give more certainty in the correlation of the different logs.

Finally it is recommended to investigate the change of the porosity and permeability with increasing distance from the crevasse channel. In this paper, it is concluded that the layers gradually change from sand layers in to silt and clay layers. At a certain point, due to this decrease in grain size, the porosity will be below the minimum required for production.

8. Acknowledgements

This research wouldn't have been possible without the help of Rick Donselaar, who gave me the opportunity to do this fieldwork. Koen van Toorenenburg, who helped me during the whole process with all my questions and Lisanne Bouman en Niels Noordijk whom I did fieldwork with and for their coorporation in the data analysis.

And furthermore I would like to thank the Molengraaff fund who gave me a grant for my field trip. And GDF Suez and EBN who make the *tough gas* project possible.

9. List of References

Banerjee, I. (1977) Experimental study on the effect of deceleration on the vertical sequence of sedimentary structures in silty sediments. *Journal of Sedimentary Petrology, Vol. 47 No. 2., 771-78*

Donselaar, M.E. and Schmidt J.M. (2005). Integration of outcrop and borehole image logs for high-resolution facies interpretation: example from a fluvial fan in the Ebro Basin, Spain. *Sedimentology, 52, 1021–1042*

Donselaar M.E. and Cueves Gozalo M.C. and Moyano, S. (2013). Avulsion processes at the terminus of low- gradient semi-arid fluvial systems: Lessons from the Río Colorado, Altiplano endorheic basin, Bolivia. *Sedimentary Geology 283 (2013), 1–14*

Fisher, J.A. and Nichols, G.J. and Waltham, D.A. (2007). Unconfined flow deposits in distal sectors of fluvial distributary systems: Examples from the Miocene Luna and Huesca Systems, northern Spain. *Sedimentary Geology 195 (2007), 55–73*

Hampton, B.A. and Horton, B.K. (2007). Sheetflow fluvial processes in a rapidly subsiding basin, Altiplano plateau, Bolivia. *Sedimentology (2007) 54, 1121–1147. doi: 10.1111/j.1365-3091.2007.00875.x*

Jones, H.L. and Hajek E.A. (2007). Characterizing avulsion stratigraphy in ancient alluvial deposits. *Sedimentary Geology 202 (2007), 124–137*

Jupp, P.E. and Spurr, B.D. and Nichols, H.J. and Hirst, J.P.P. (1987). Statistical estimation of the apex of a sediment distribution system from paleocurrent data. *Mathematical Geology, Volume 10, Issue 4, May 198, 319-333*

Nichols, G. (2005). Tertiary alluvial fans at the northern margin of the Ebro Basin: a review. *Geological Society, London, Special Publications 2005, v.251, 187-206, doi: 10.1144/GSL.SP.2005.251.01.13*

Nichols, G.J. and Fisher, J.A. (2007). Processes, facies and architecture of fluvial distributary system deposits. *Sedimentary Geology 195 (2007), 75–90*

Nichols, G.J. and Hirst, J.P. (1998). Alluvial fans and fluvial distributary system, oligo-miocene, Northern Spain: Contrasting processes and products. Journal of Sedimentary Research, volume 68, issue 5, 879-889.

Torres Carranza, Y.A. (2013). Static reservoir model of crevasse splays in the Colorado river system, Salar of Uyuni, Bolivia. *MSc Thesis, Delft University of Technology, Delft, the Netherlands, 135 pp.*

Appendices

Appendix A: Logs of level 5, at the Dam outcrop

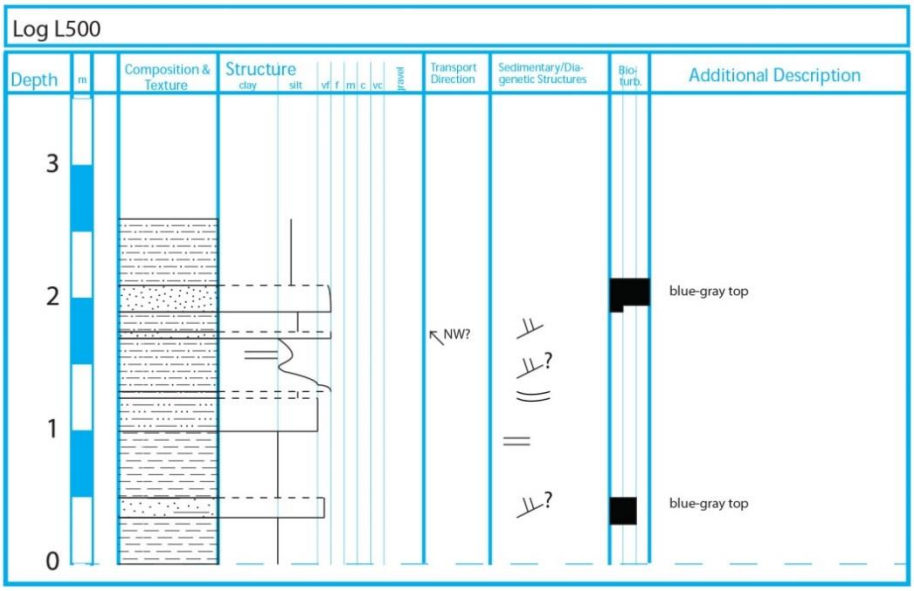

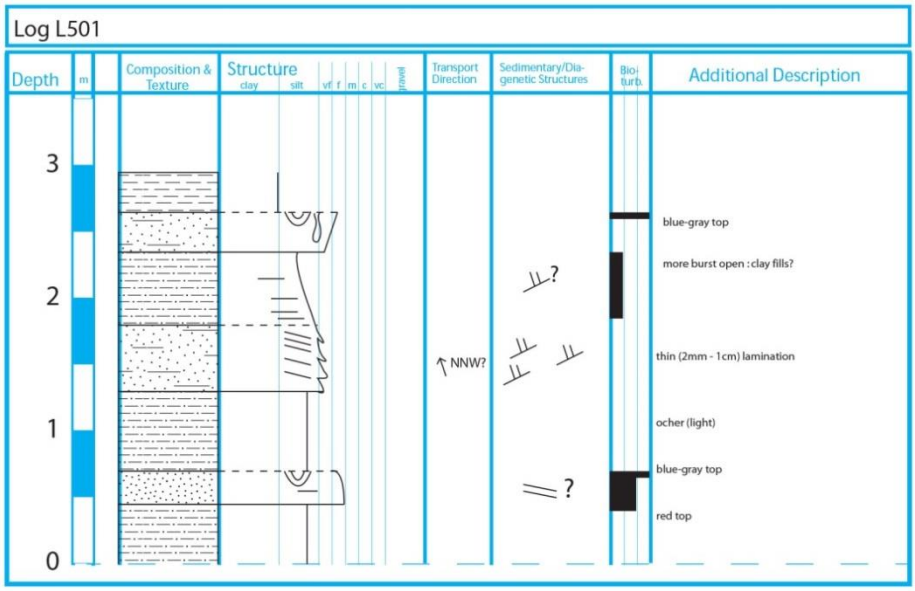

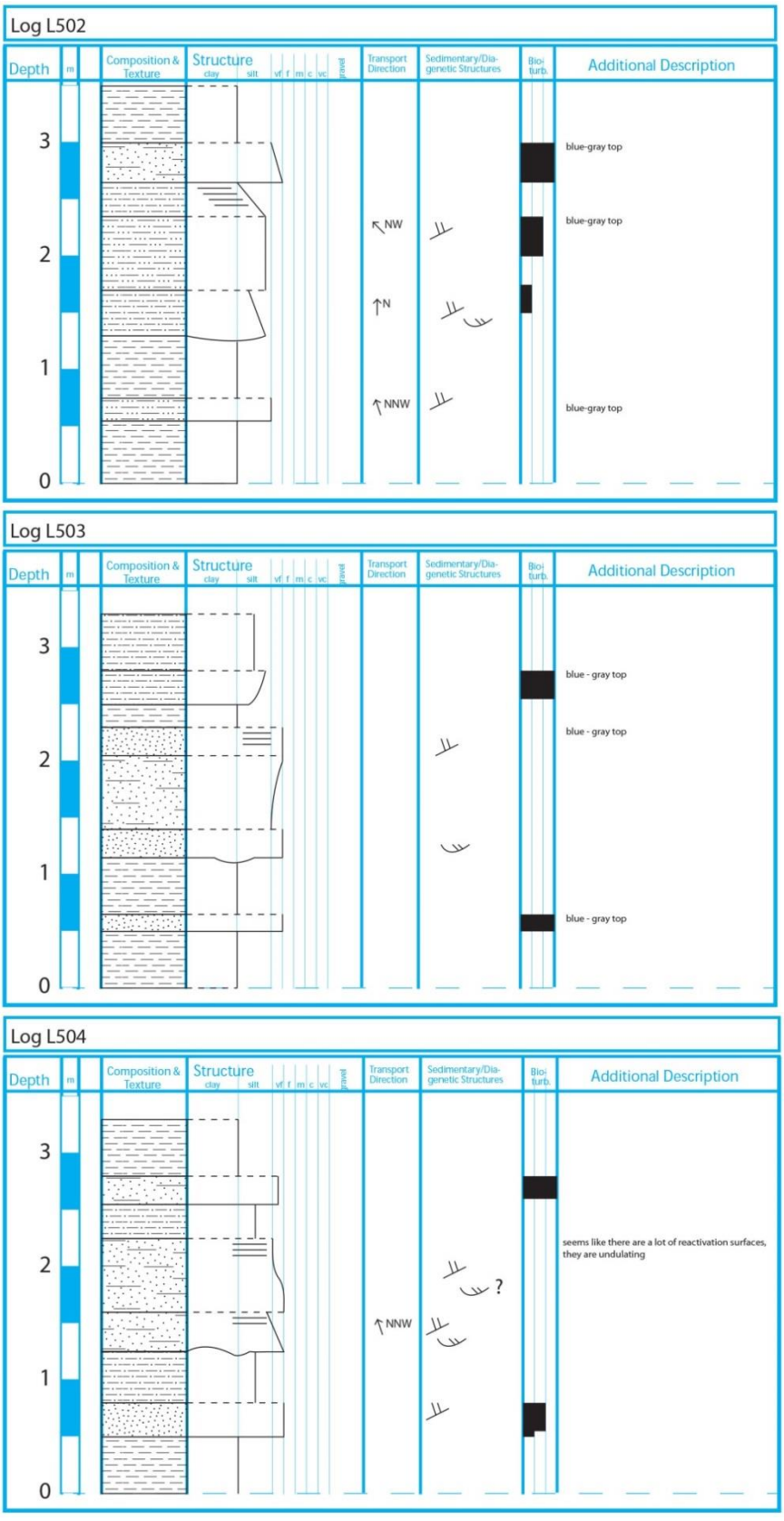
Log L502
Depth
m
Composition & Texture
Structure
clay
silt
vf
f
m
c
vc
gravel
Transport Direction
Sedimentary/Dia-genetic Structures
Bio-turb.
Additional Description
3
2
1
0
NW
N
NNW
blue-gray top
blue-gray top
blue-gray top
Log L503
Depth
m
Composition & Texture
Structure
clay
silt
vf
f
m
c
vc
gravel
Transport Direction
Sedimentary/Dia-genetic Structures
Bio-turb.
Additional Description
3
2
1
0
blue - gray top
blue - gray top
blue - gray top
Log L504
Depth
m
Composition & Texture
Structure
clay
silt
vf
f
m
c
vc
gravel
Transport Direction
Sedimentary/Dia-genetic Structures
Bio-turb.
Additional Description
3
2
1
0
NNW
?
seems like there are a lot of reactivation surfaces, they are undulating

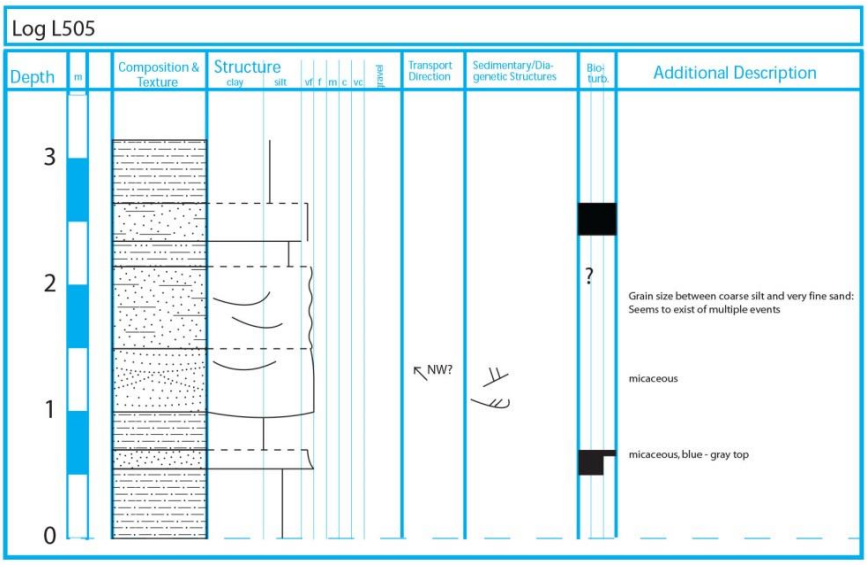
Log L505
Depth
m
Composition & Texture
Structure
clay
silt
vf
f
m
c
vc
gravel
Transport Direction
Sedimentary/Dia-genetic Structures
Bio-turb.
Additional Description
3
2
1
0
NW?
?
Grain size between coarse silt and very fine sand: Seems to exist of multiple events
micaceous
micaceous, blue - gray top

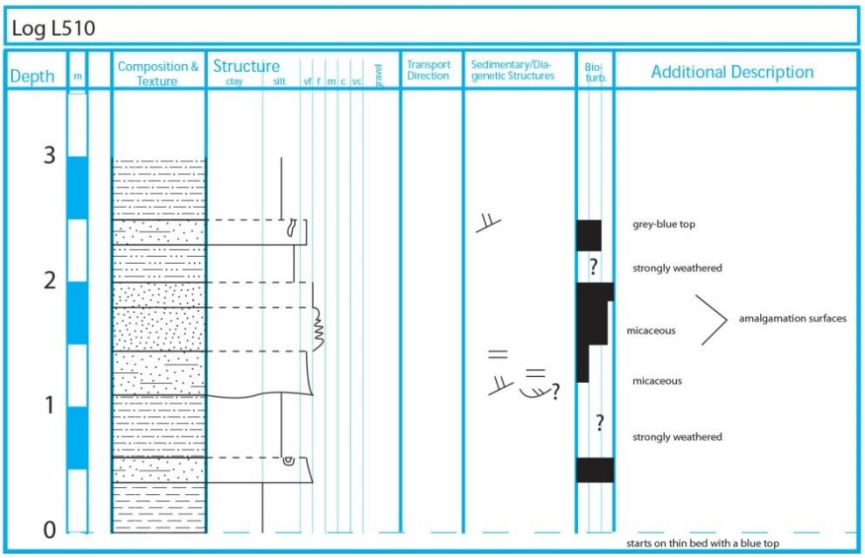
Log L510
Depth
m
Composition & Texture
Structure
clay
silt
vf
f
m
c
vc
gravel
Transport Direction
Sedimentary/Dia-genetic Structures
Bio-turb.
Additional Description
3
2
1
0
?
?
?
grey-blue top
strongly weathered
micaceous
amalgamation surfaces
micaceous
strongly weathered
starts on thin bed with a blue top

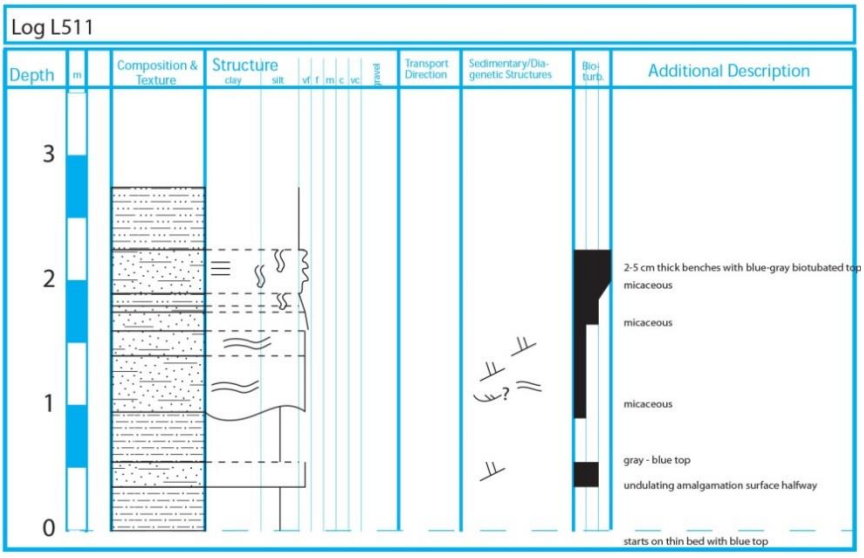
Log L511
Depth
m
Composition & Texture
Structure
clay
silt
vf
f
m
c
vc
gravel
Transport Direction
Sedimentary/Dia-genetic Structures
Bio-turb.
Additional Description
3
2
1
0
?
2-5 cm thick benches with blue-gray biotubated top
micaceous
micaceous
micaceous
gray - blue top
undulating amalgamation surface halfway
starts on thin bed with blue top

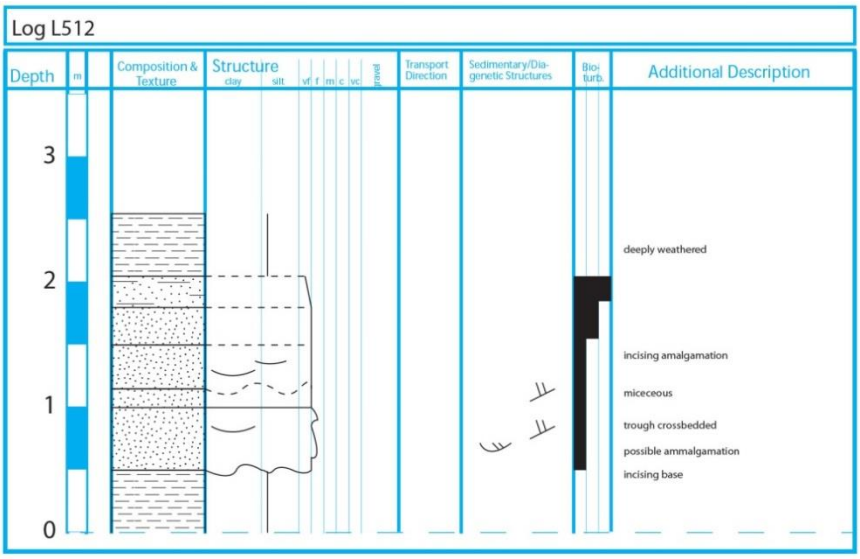
Log L512
Depth
m
Composition & Texture
Structure
clay
silt
vf
f
m
c
vc
gravel
Transport Direction
Sedimentary/Dia-genetic Structures
Bio-turb.
Additional Description
3
2
1
0
deeply weathered
incising amalgamation
miceceous
trough crossbedded
possible ammalgamation
incising base

Appendix B: Logs of level 10

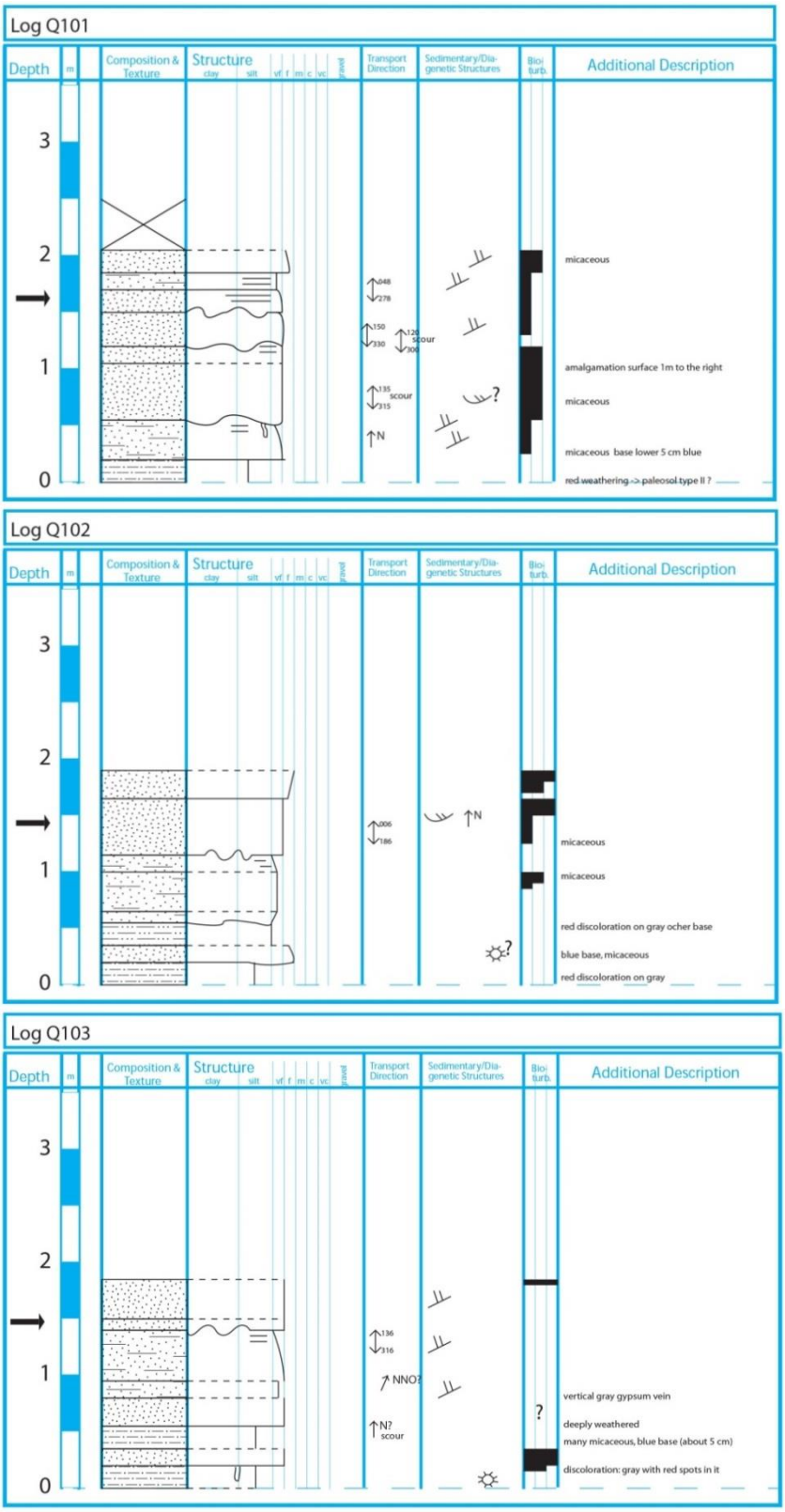

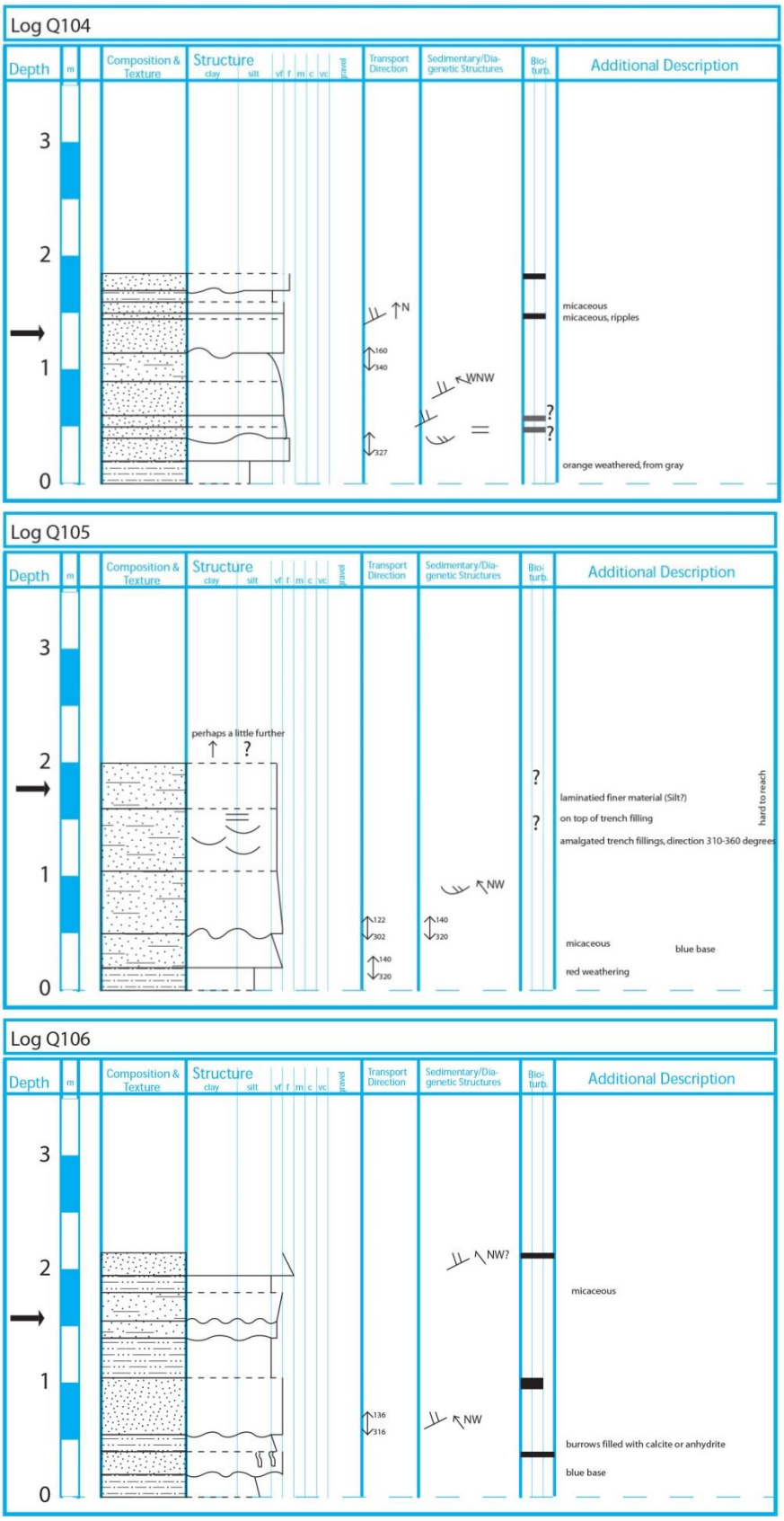
Log Q104
Depth
m
Composition & Texture
Structure
clay
silt
vf
f
m
c
vc
gravel
Transport Direction
Sedimentary/Dia-genetic Structures
Bio-turb.
Additional Description
3
2
1
0
N
160
340
327
WNW
micaceous
micaceous, ripples
orange weathered, from gray
Log Q105
perhaps a little further
NW
122
302
140
320
laminatied finer material (Silt?)
on top of trench filling
amalgated trench fillings, direction 310-360 degrees
hard to reach
micaceous
blue base
red weathering
Log Q106
NW?
NW
136
316
micaceous
burrows filled with calcite or anhydrite
blue base

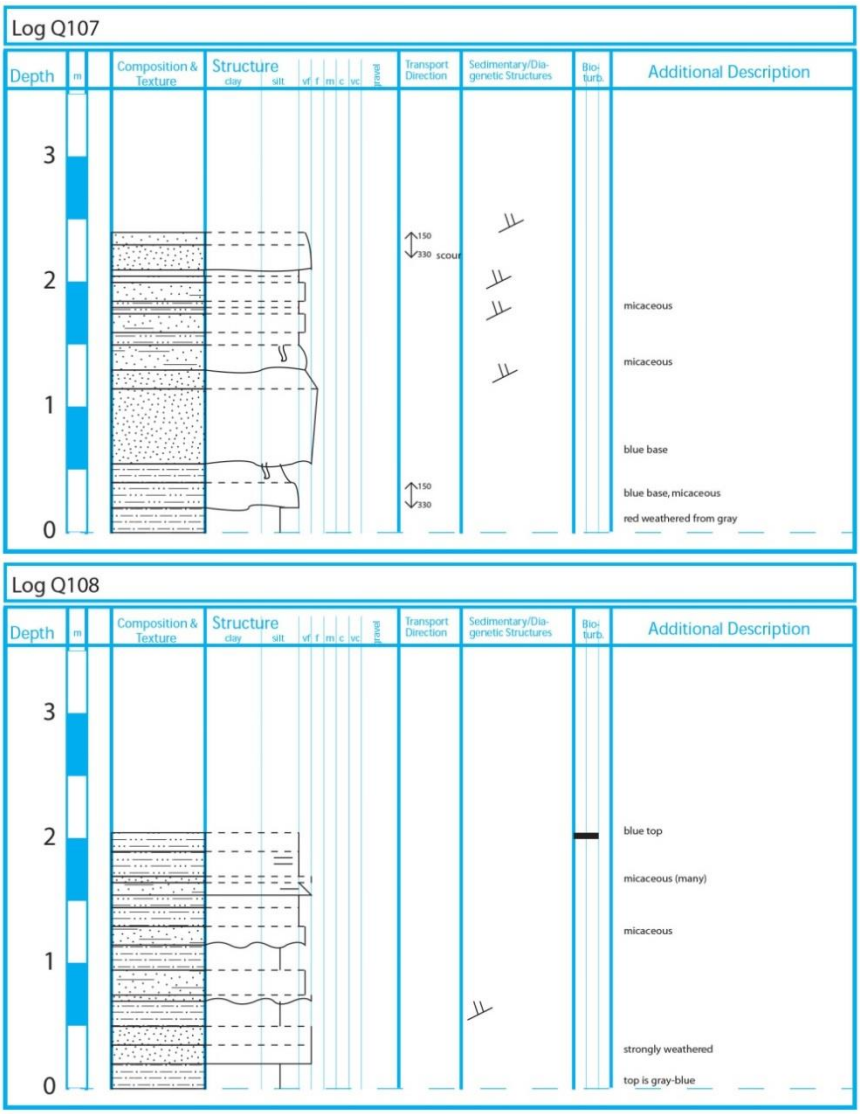
Log Q107
Depth
m
Composition & Texture
Structure
clay
silt
vf
f
m
c
vc
gravel
Transport Direction
Sedimentary/Dia-genetic Structures
Bioturb.
Additional Description
3
2
1
0
150
330
scour
150
330
micaceous
micaceous
blue base
blue base, micaceous
red weathered from gray
Log Q108
Depth
m
Composition & Texture
Structure
clay
silt
vf
f
m
c
vc
gravel
Transport Direction
Sedimentary/Dia-genetic Structures
Bioturb.
Additional Description
3
2
1
0
blue top
micaceous (many)
micaceous
strongly weathered
top is gray-blue

Appendix C: Correlation cross-sections of level 10

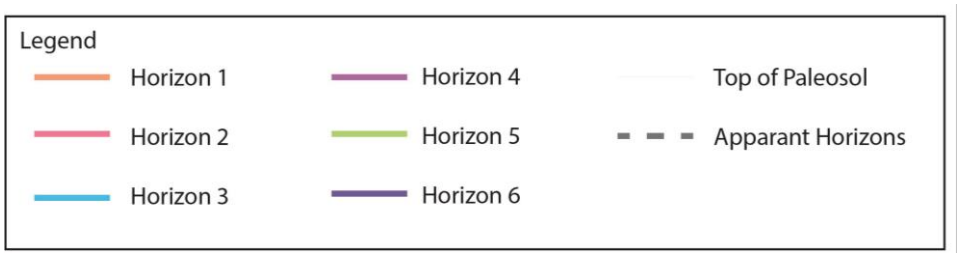

Figure 34. Legend of the horizons in the Log correlation cross-sections.

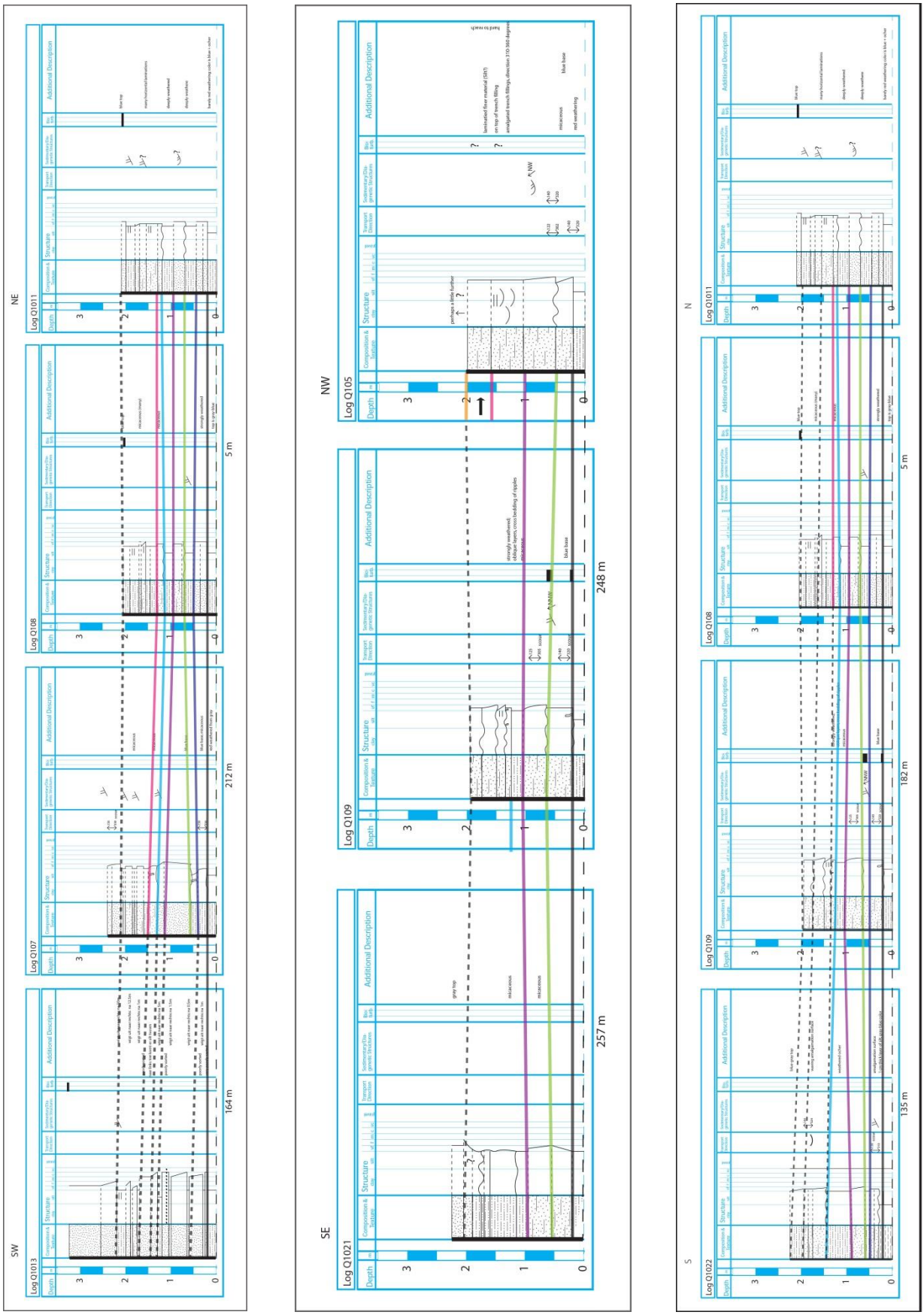
SW
NE
SE
NW
S
N
Log Q1013
Log Q107
Log Q108
Log Q1011
Log Q1021
Log Q109
Log Q105
Log Q1022
164 m
212 m
5 m
257 m
248 m
135 m
182 m
5 m
Depth
Composition & Texture
Structure
Transport Direction
Sedimentary/Biogenic Structures
Bio. turb.
Additional Description

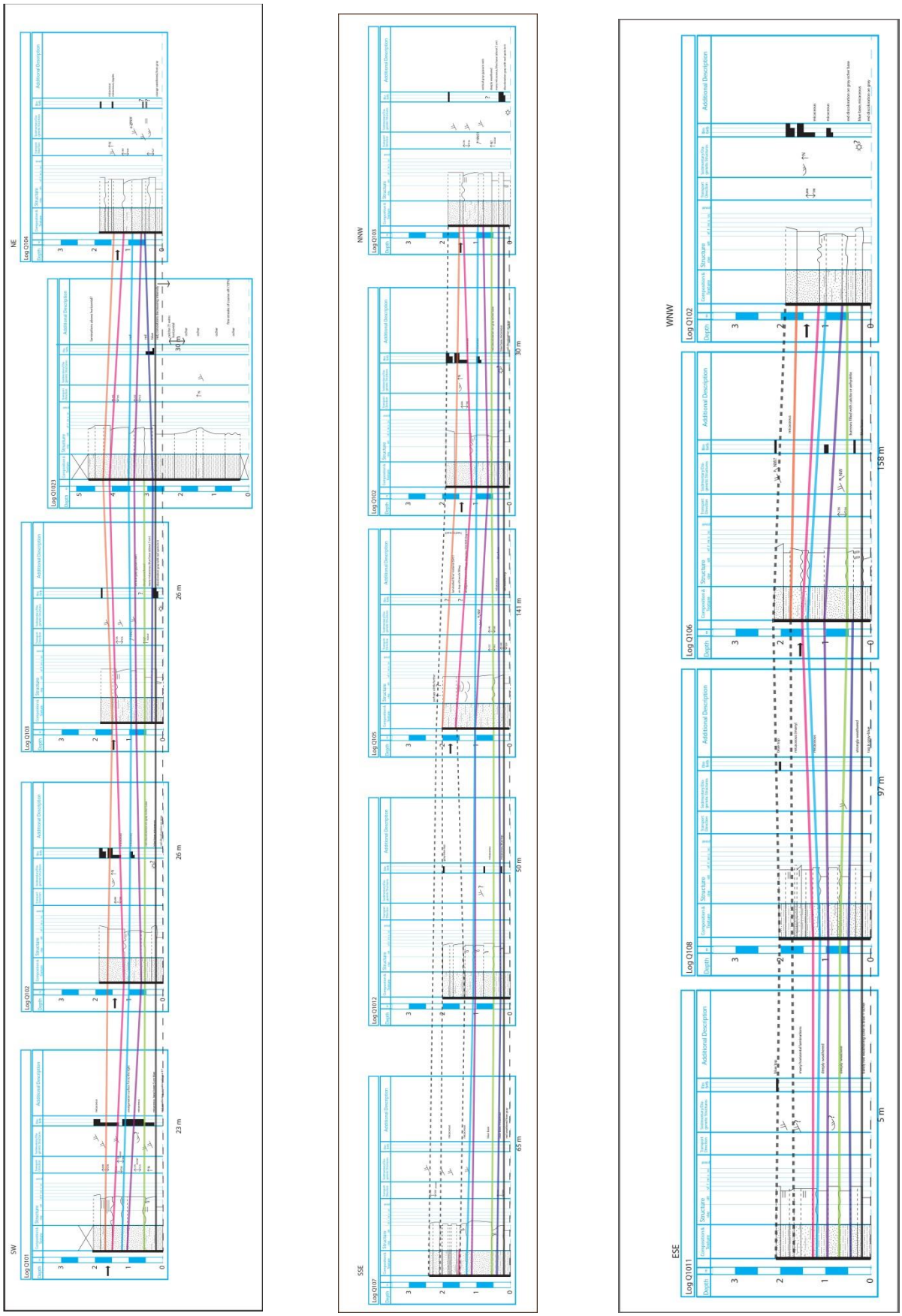
SW
NE
SSE
NNW
ESE
WNW
Log Q101
Log Q102
Log Q103
Log Q104
Log Q105
Log Q106
Log Q107
Log Q108
Log Q1011
Log Q1012
Log Q1023
23 m
26 m
26 m
30 m
65 m
50 m
141 m
158 m
97 m
5 m

Appendix D: Schematic grain size distributions of level 10

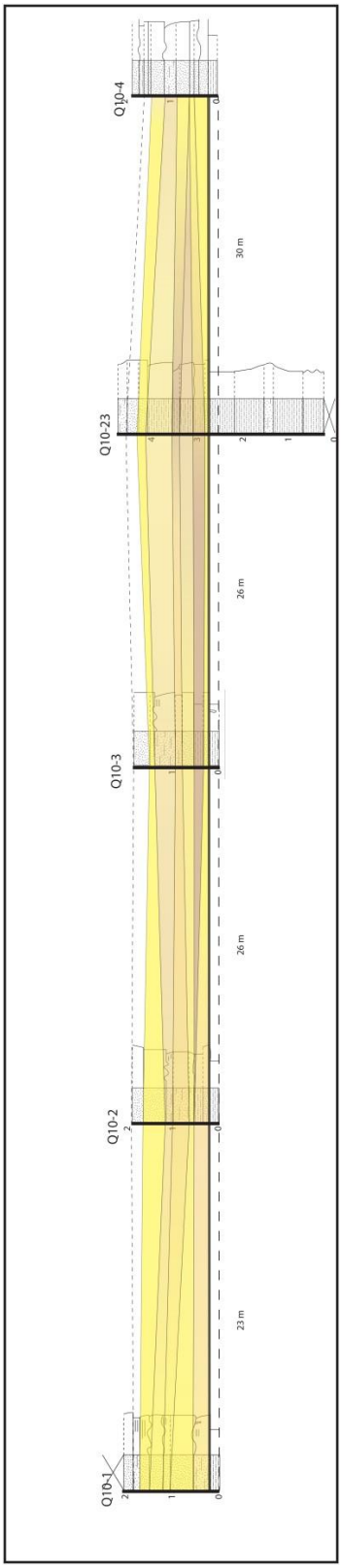

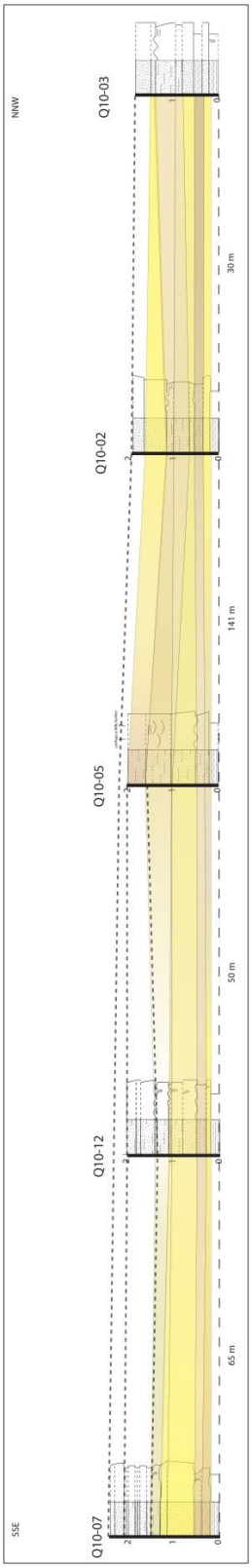

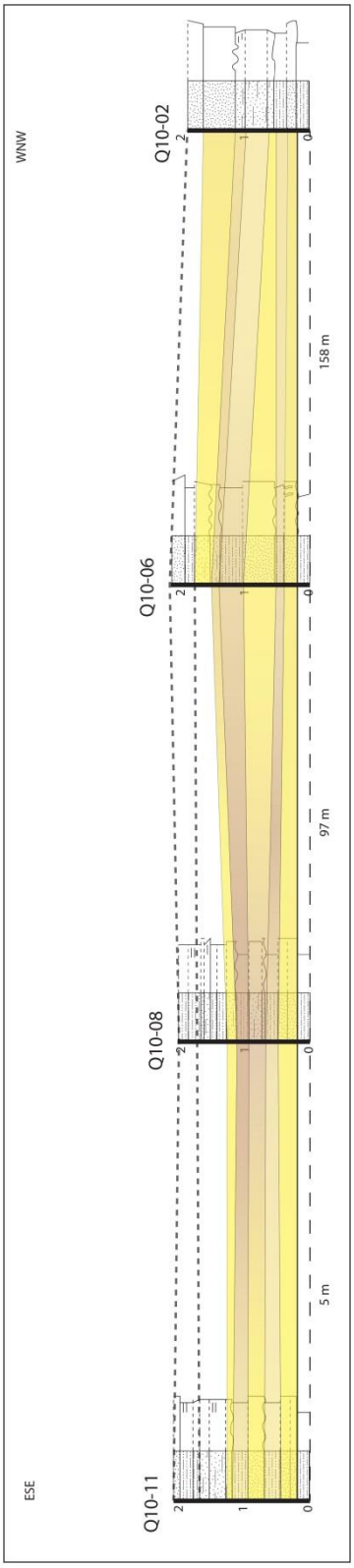

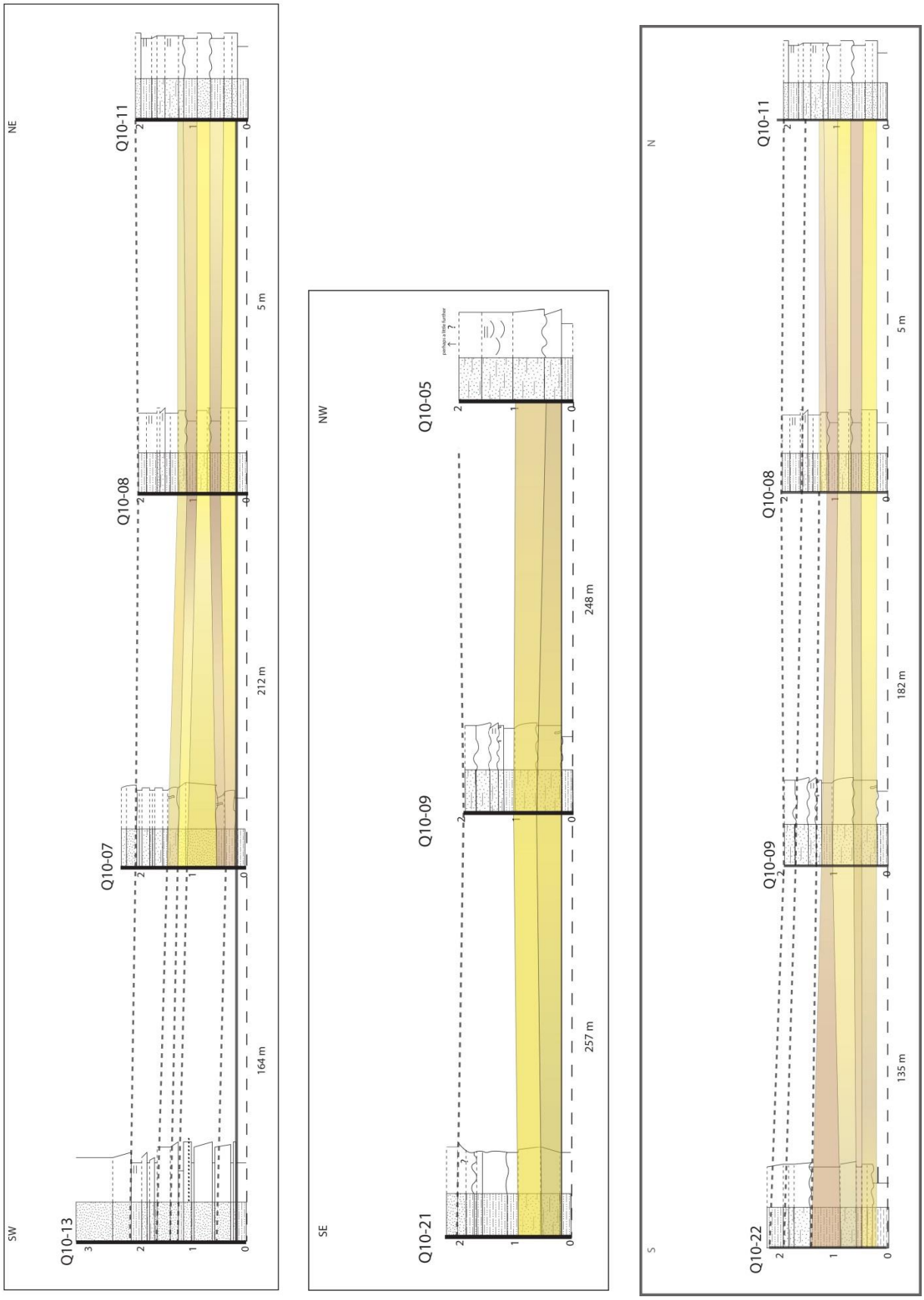
NE
SW
Q10-11
Q10-08
Q10-07
Q10-13
5 m
212 m
164 m
NW
SE
Q10-05
Q10-09
Q10-21
248 m
257 m
N
S
Q10-11
Q10-08
Q10-09
Q10-22
5 m
182 m
135 m

Appendix E: Enlarged map of the Quicena outcrop

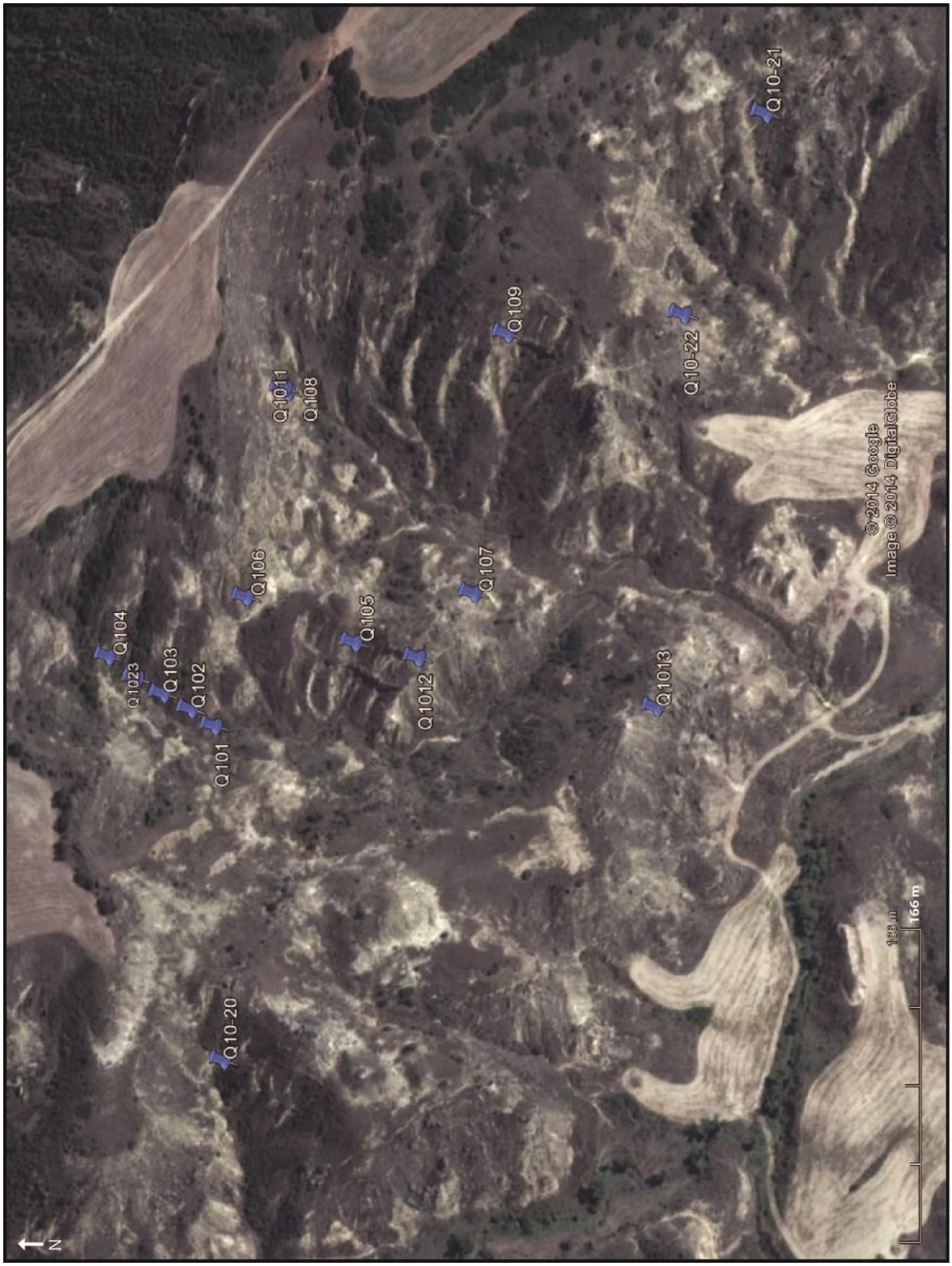

Appendix F: Enlarged map of the Dam outcrop

Appendix G: STGIIP calculation sheet

Gas Initially in Place (GIIP) vs. Stock Tank Gas Initially in place (STGOIP)

*Example considering a Crevasse splay deposit of 5x5 km area and thickness of 20cm.
Porosity of 20% with a high Net to gross ratio of 0.80 and a Gas saturation of 80%.
** Reservoir conditions considered are: 80 Degrees Celcius (176F) and 200 Bar (2900psia)

INPUTS				
Thickness	H	0,8	[m]	
Area	A	85038	[m^2]	
Porosity	ϕ	0,2	[fraction]	
Net to Gross	N/G	0,7	[fraction]	
Water Saturation	S_w	0,2	[fraction]	
Reservoir Temp.	T_{res}	80	[Celsius]	
Reservoir Pess.	P_{res}	200	[Bar]	
PseudoCritical Press	P_{pc}	663,3	[Psia]	READ COMMENT - BOTH ARE DEPENDANT ON
PseudoCriticalTemp	T_{pc}	374,1	[Rankine]	THE GAS COMPOSITION
PRE-CALCULATIONS (AUTOMATIC)				
Rock Bulk Volume	RBV	68030,4	[m^3]	
Reservoir Press.	P_{res}	2900,75	[Psia]	
Reservoir Temp.	T_{res}	635,67	[Rankine]	
Reservoir Temp.	T_{res}	176	[Farenheit]	
Reduced Res. Press	P_{pr}	4,37		$P_{pr}=\frac{P_{res}[psia]}{P_{pc}[psia]}$
Reduced Res. Temp	T_{pr}	1,70		$T_{pr}=\frac{T_{res}[psia]}{T_{pc}[psia]}$
Z-factor @ Res. Cond.	Z_{res}	0,82	[-]	READ COMMENT - IS MANUALLY CALCULATED FROM GRAPH ONLY IF PSEUDO CRITICAL PRES. AND TEMP. ARE KNOWN
CALCULATIONS (AUTOMATIC)				
Expansion Factor	E_{gi}	196,83	[vol/vol]	$E_g=35.37\cdot\frac{P_{res}[psia]}{Z_{res}T_{res}[Rankine]}$
Gas Formation Factor	B_{gi}	0,00508		
Gas initially in Place	**GIIP**	**52963503,4**	**cu.f**	$GIIP\ [ft^3]=\frac{35.31467 ft^3}{1m^3}\cdot RBV[m^3]\cdot\varphi\cdot N/G\cdot(1-S_w)\cdot E_g$
Gas initially in Place	**GIIP**	**53**	**10^6 cu.f**	
Gas initially in Place	**GIIP**	**0**	**BCF**	

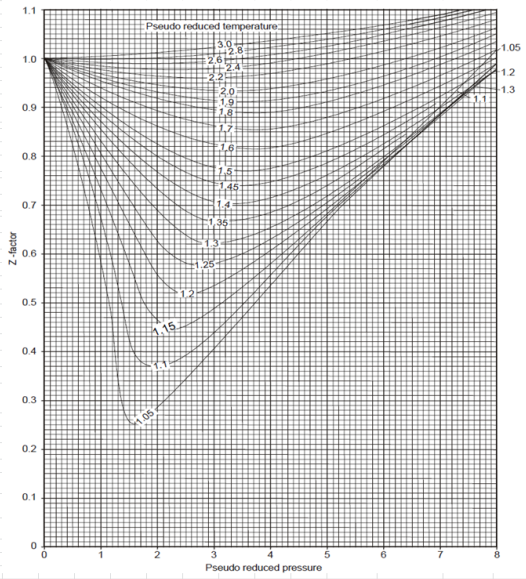

Gas Initially in Place (GIIP) vs. Stock Tank Gas Initially in place (STGOIP)

*Example considering a Crevasse splay deposit of 5x5 km area and thickness of 20cm.
Porosity of 20% with a high Net to gross ratio of 0.80 and a Gas saturation of 80%.
** Reservoir conditions considered are: 80 Degrees Celcius (176F) and 200 Bar (2900psia)

INPUTS				
Thickness	H	0,8	[m]	
Area	A	493022	[m^2]	
Porosity	ϕ	0,2	[fraction]	
Net to Gross	N/G	0,7	[fraction]	
Water Saturation	S_w	0,2	[fraction]	
Reservoir Temp.	T_{res}	80	[Celsius]	
Reservoir Pess.	P_{res}	200	[Bar]	
PseudoCritical Press	P_{pc}	663,3	[Psia]	READ COMMENT - BOTH ARE DEPENDANT ON
PseudoCriticalTemp	T_{pc}	374,1	[Rankine]	THE GAS COMPOSITION
PRE-CALCULATIONS (AUTOMATIC)				
Rock Bulk Volume	RBV	394417,6	[m^3]	
Reservoir Press.	P_{res}	2900,75	[Psia]	
Reservoir Temp.	T_{res}	635,67	[Rankine]	
Reservoir Temp.	T_{res}	176	[Farenheit]	
Reduced Res. Press	P_{pr}	4,37		$P_{pr}=\frac{P_{res}[psia]}{P_{pc}[psia]}$
Reduced Res. Temp	T_{pr}	1,70		$T_{pr}=\frac{T_{res}[psia]}{T_{pc}[psia]}$
Z-factor @ Res. Cond.	Z_{res}	0,82	[-]	READ COMMENT - IS MANUALLY CALCULATED FROM GRAPH ONLY IF PSEUDO CRITICAL PRES. AND TEMP. ARE KNOWN
CALCULATIONS (AUTOMATIC)				
Expansion Factor	E_{gi}	196,83	[vol/vol]	$E_g=35.37\cdot\frac{P_{res}[psia]}{Z_{res}T_{res}[Rankine]}$
Gas Formation Factor	B_{gi}	0,00508		
Gas initially in Place	**GIIP**	**307064752**	**cu.f**	$GIIP\ [ft^3]=\frac{35.31467 ft^3}{1m^3}\cdot RBV[m^3]\cdot\varphi\cdot N/G\cdot(1-S_w)\cdot E_g$
Gas initially in Place	**GIIP**	**307**	**10^6 cu.f**	
Gas initially in Place	**GIIP**	**0**	**BCF**